10

**15** 

**₩**20

Ш

Ñ25

30

# COMPOSITION AND METHOD FOR THE ENHANCEMENT THE EFFICACY OF

್ಟ್ರಾರ್ಡ್ ಆರ್.೨ ರಾಜ್ಯ್ ಕ The present invention relates to the enhancement of the efficacy of drugs, and more particularly, with overcoming the resistance of cells or organisms to drugs.

### BACKGROUND TO THE INVENTION

The clinical usefulness of any chemotherapeutic agent or drug can be severely affected by the emergence of cellular resistance to that drug. Accordingly, a significant amount of research has been conducted in an attempt to elucidate the cellular mechanisms involved with resistance to drugs, as well as methods for overcoming such resistance. To date a number of putative cellular mechanisms involved in drug resistance have been proposed. These include:

- (i) altered metabolism of the drugs, which could include decreased activation or increased deactivation;
- (ii) impermeability of the target cell or organism to the active compound;
  - (iii) altered specificity of an inhibited enzyme;
  - (iv) increased production of a target molecule;
  - increased repair of cytotoxic lesions; and
- (vi) bypassing of an inhibited reaction by alternative biochemical pathways.

The cellular mechanisms involved in drug resistance are complex, and consequently there has been little progress in the development of generally applicable methods for overcoming drug resistance problems. A further complicating factor is that while drug resistance is a problem associated with nearly all chemotherapeutic applications, it is more often associated with diseases 35 which require on-going and prolonged treatment with a number of concurrent drugs.

In cancer treatment, for example, impermeability

al., 1989).

Q

ti.

W

3

**L** 

ليا

25

30

35

resistance.



of the cancer cells to the active compound is often observed. Moreover, it is often found that resistance to one drug may confer resistance to other biochemically distinct drugs. This has been termed multidrug resistance.

- 5 Drugs that are typically affected by the multidrug
  resistance problem include doxorubicin, vincristine,
  vinblastine, colchicine and actinomycin D. In at least
  some cases, multidrug resistance is a complex phenotype
  that has been linked to a high level of expression of a
  10 cell membrane drug efflux transporter called MdrI protein,
  also known as P-glycoprotein. This membrane "pump" has
  broad specificity, and acts to remove from the cell a wide
  variety of chemically unrelated toxins (see Endicott et
- Recently, a similar mechanism of broad-spectrum drug resistance has been reported for certain microorganisms. These results indicate the existence of bacterial efflux systems of extremely broad substrate specificity that are similar to the multidrug resistance pump of mammalian cells (see Nikaido, 1993).

Substances which reverse multidrug resistance are known as resistance modification agents (RMAs), and are of importance in potentiating the cytotoxicity of chemotherapeutic agents to which a human cancer has become resistant. Although many agents have been identified as RMAs in vitro, a large proportion of these have little or no therapeutic potential because of high toxicity in vivo at the doses required to reverse multidrug resistance. For example, metabolic poisons, such as azide, are able to reverse multidrug resistance in vitro, but have no usefulness in vivo. Most other highly effective RMAs, such as PSC833, appear to work as competitive antagonists of a drug-binding site on the MdrI protein. Many of these agents also have toxicity that limits their usefulness in vivo.

Consequently, there is a need to develop alternate

pharmacological strategies for reversing multidrug

than et alcurente (20)

30

35

10

In an attempt to overcome poor tumour uptake of anti-neoplastic drugs and reduce systemic toxicity (Singh et al. 1991), investigators have attempted to target antineoplastic drugs such as methotrexate (MTX) to the docation of malignant stissue. 22 Several studies have already for attempted to target chemotherapeutic agents to tumours by linking drugs to polymers selected for their affinity to tumours (Hudecz et al., 1993; Klein et al., 1994; Akima et al., 1996). However, while these polymers may help to deliver active agents to their target tissues, they do not necessarily overcome the drug resistance problem.

One polymer which has been proposed as a tumour targeting agent is hyaluronan (HA). HA, also known as hyaluronic acid, is a naturally occurring polysaccharide comprising linear-chain polymers, which is found ubiquitously throughout the animal kingdom. HA is highly water-soluble, making it an ideal drug delivery vehicle for biological systems.

The applicants have now surprisingly found that HA exhibits unique structural and physicochemical properties which not only enhance its usefulness as a drug carrier, but also aid in overcoming drug resistance. high concentrations of ~1g/L, HA adopts a stiffened random coil configuration that occupies an exceptional volume relative to molecule mass (Laurent, 1970), and at this level or below, it forms loose links to macromolecular networks (Figure 1). While not wishing to be bound by any particular theory, we consider that, based on the physical characteristics of HA, the mechanism of interaction between polysaccharide and agents such as methotrexate, may take one or both of two forms:

Chemical Interaction (Figure 2A).

Ionic bonding could occur between the MTX amine groups and the HA carboxyl groups, but such an interaction could cause precipitation. Another possible interaction is via hydrogen bonding between available amine groups on the drug and hydroxyl groups of the HA, but this is unlikely

20

25

30

35

because methotrexate is relatively insoluble in water; therefore if this were to occur it would be a very weak interaction. The most likely bonding between MTX and HA would be via hydrophobic interactions between MTX's 5.5 numerous hydrophobic groups and the hydrophobic patches in the secondary structure of HAP (Scotter al : 1989).

Tight are page ( ) (ii) Molecular Association as an exerce to Where MTX is merely "mixed" in HA gel (Figure 2B) with no specific chemical bond formation, MTX could become entrapped within the 3-dimensional meshwork formed by higher concentrations of HA (Mikelsaar and Scott, 1994), so that the drug simply diffuses from the HA after administration. If HA is rapidly taken up and bound by specific cell receptors, the drug will be released in

higher concentration at these points eg. lymph nodes, 15 liver, bone marrow, tumour cells with HA receptors.

While again not wishing to be bound by any particular theory, one mechanism by which HA helps to target active agents may be via the characteristic overexpression of HA receptors in several tumour types (Stamenkovic et al., 1991; Wang et al., 1998). The HA receptors CD44, Receptor for Hyaluronan Mediated Motility (RHAMM) and ICAM-1, have been linked to tumour genesis (Bartolazzi et al., 1994) and progression (Günthert 1993; Arch et al., 1992). RHAMM is a major factor in mediating tumour cell motility and invasion (Hardwick et al., 1992). It has been demonstrated that RHAMM is required for H-ras transformation of fibroblasts (Hall et al., 1995), which would make this receptor a potential participant in tumour formation and growth. ICAM-1, a receptor tentatively linked to HA metabolism (McCourt et al., 1994), is highly expressed in transformed tissues such as mouse mastocytomas (Gustafson et al., 1995a) and in the stroma and clusters of tumour cells of human breast carcinomas (Ogawa et al., 1998).

Increased expression of HA receptors on tumour cells provides a rationale for attempting the incorporation □ 15 ©

N

Ų.

**1** 25

30

35

**20** 

of HA into chemotherapeutic treatment regimens. However, the very limited data obtained to date actually teach away from the presently claimed process. For example, limited success has been obtained by chemically complexing HA to mitomycin C and epirubicin; investigators were able to inhibit colon carcinoma growth by 0.8-25% (Akima et al., 1996). Klein and colleagues (1994) reported an increased uptake of the drug into implanted rat mammary and Fischer bladder carcinomas was achieved by merely mixing HA with 5-10 FU. Mouse mastocytomas were also demonstrated to have an affinity for intravenously-injected HA (Gustafson et al., 1995b).

However, while some of the HA research has shown that HA can be used as a drug carrier, none of this research has shown that HA is capable of overcoming cellular resistance to drugs.

### SUMMARY OF THE INVENTION

The present invention provides a method for enhancing the effectiveness of a cytotoxic or antineoplastic agent, comprising the step of co-administering said agent with hyaluronan, wherein co-administration with hyaluronan enhances the agent's cancer cell-killing potential.

Typically, co-administration of a cytotoxic or anti-neoplastic agent with hyaluronan enhances its cancer cell-killing potential. That is, cancer cells that are normally resistant to the drug become susceptible to it.

Preferably, the agent is methotrexate, paclitaxel (taxol) or 5-fluorouracil (5-FU).

According to a second aspect of the present invention there is provided a cytotoxic or anti-neoplastic pharmaceutical composition comprising hyaluronan and a cytotoxic or anti-neoplastic agent. Optionally,

conventional pharmaceutical adjuncts may be included in the pharmaceutical composition.

Typically said drug is entrained within or bound

W

20

25

to hyaluronan.

According to a third aspect of the present invention there is provided a method of enhancing the effectiveness of a cytotoxic or anti-neoplastic agent,

- composition comprising hyaluronan and said agent.
- believed possible mechanisms for overcoming drug resistance are:
- 10 1. Hyaluronan binds to receptors on the resistant cell or enters the cell via bulk endocytosis, resulting in the entrained or bound agent being delivered into the cell, allowing it to become therapeutically active.
- 2. Hyaluronan binds to the surface of the resistant cell, where the entrained or bound agent diffuses from the hyaluronan meshwork into the cell, resulting in the agent being delivered to the resistant cell.
  - 3. Hyaluronan and other mucopolysaccharides adopt a coiled configuration that entrains the agent, and may also bind a variety of agents.

Accordingly in a fourth aspect, the present invention provides a method of reducing or overcoming drugresistance, comprising the step of co-administering a cytotoxic or anti-neoplastic agent with a

- mucopolysaccharide capable of entraining and/or binding said agent and capable of binding to receptors on the resistant cell or entering the cell via bulk endocytosis, wherein said agent is delivered into the cell, thereby allowing it to become therapeutically active.
- While not wishing to be bound by theory, it may also be that a combination of hyaluronan with a drug results in the drug being retained in the cell for a longer period, allowing a prolonged release and more time for the drug to exert its pharmacological effect.
- Accordingly, in the fifth aspect of the present invention there is provided a method for enhancing the effectiveness of a drug, comprising the step of co-

10

ι.

□15

II.

**-**

L.

□ П<sub>25</sub>

30

35

69 1 1 1 1 Tell

administering said drug with a mucopolysaccharide which associates with said drug in such a manner that said drug is retained in the cell for a longer period than if said drug were administered alone. For example, where the drug is a cytotoxic drug, the drug will be retained in the cell for a longer period, allowing a prolonged release and more time to exert its toxic effects.

According to a sixth aspect of the present invention there is provided a method for the treatment of a drug-resistant disease, comprising the step of coadministering hyaluronan and a drug to a patient in need of such treatment.

In one embodiment, this aspect of the invention provides a method for the treatment of a drug resistant disease, comprising the step of administering a composition comprising hyaluronan and a drug to a patient in need of such treatment.

In particular, the method for treatment of a drug resistant disease is applicable to a patient with a drug resistant cancer. Preferably, the cancer is resistant to methotrexate or 5-FU.

More preferably, said drug resistance is multidrug resistance.

According to an seventh aspect of the present invention there is provided a method for the treatment of cancer, comprising the step of co-administering a drug and a mucopolysaccharide capable of entraining or binding said drug and/or associating with said drug in such a manner that said drug is retained in a cancer cell for a longer period than if said drug were administered alone.

According to an eighth aspect of the present invention there is provided a method for the reduction of gastrointestinal toxicity of a drug, comprising the step of co-administering a drug and a mucopolysaccharide capable of entraining or binding said drug and/or associating with said drug in such a manner that said drug has reduced gastrointestinal toxicity.

30

35

Throughout the description and claims of this specification, the word "comprise" and variations of the word, such as "comprising" and "comprises", means "including but not limited to" and is not intended to exclude other additives, components, integers or steps.

# BRIEF DESCRIPTION OF THE FIGURES DESCRIPTION OF

Figure 1 shows that in higher concentrations HA forms a three-dimensional meshwork which is capable of entraining small molecules such as methotrexate. The 10 HA/drug targeting of pathological sites is accomplished by the HA rapidly binding to specific cell receptors, followed by diffusion of the drug from the HA, and/or cointernalization of both the HA and drug via HA and/or drug receptors.

Figure 2A shows the possible molecular interactions between methotrexate and HA. These include (i) ionic bonding, (ii) hydrogen bonding or (iii) hydrophobic bonding.

20 Figure 2B is a diagrammatic representation of the entanglement of methotrexate in HA. At higher concentrations HA forms a 3-dimensional meshwork which is represented by the large coiled molecule. (\*) represents the methotrexate which has a molecular weight of only 454D, and is easily entrained in the 400-900 kD HA molecule. 25

Figure 3 shows the general pathology of human breast cancer tumours grown in nude mice. Panel A shows the general morphology of a grade II-III human tumour. Panel B shows a micrograph of another section of the tumour exhibited in Figure 3A. This section shows the surrounding mouse muscle (M), tumour capsule (C), necrotic areas of the tumour (N), infiltrating tumour (T) and  $(\Rightarrow)$  indicates a common phenomenon known as "Indian files", in which carcinoma cells line up in files which are often associated with an infiltrating carcinoma (Carter, 1990).

Figure 4 shows the classical pathological features of breast malignancy. Panel A shows a section of

10

1.

1

· 🖺 20

o L

142

Ū 25

30

35

□ 15

characteristic infiltrating duct carcinoma with large areas of necrosis (N), indicating the more aggressive course of the tumour. Panel B shows the presence of blood cells (), demonstrating that the tumour is vascularized and therefore viable. In close proximity to the blood vessel there are a few observed ducts (D). Panel C shows cells, labelled as (A), undergoing apoptosis, as indicated by the nuclear fragmentation.

Figure 5 shows the immunohistochemical identification of HA receptors on the human breast cancer tumours grown in nude mice. Panel A shows carcinoembryonic antigen (CEA) localisation in tumour. Panel B shows RHAMM expression on human breast carcinoma. Panel C shows ICAM-1 expression on human breast carcinoma. The localisation of HA receptor, ICAM-1 is primarily around endothelial tissue (→). Panel D shows CD44 expression on human breast carcinoma. CD44H was detected on approximately 95% of the tumour cells. H: cells of human origin; M: cells of murine origin.

Figure 6 shows the results of molecular weight analysis of hyaluronan used as a carrier for the methotrexate targeting of tumours.

Figure 7 shows methotrexate targeting of human breast cancer tumours, using HA as a carrier.

Figure 8 shows enhanced uptake of methotrexate in the liver in the presence of HA.

Figure 9 shows reduced uptake of methotrexate in the gastrointestinal tract when drug is administered with HA.

Figure 10 shows a diagrammatic representation of possible physical interactions between MTX/HA and subsequent tumour targeting abilities of the drug/HA combination therapy.

Figure 11 shows the cytotoxic synergistic in vitro effect of combining HA with 5-FU.

Figure 12 shows 5-FU targeting of human breast cancer tumours using HA as a carrier.

20

35

Figure 13 shows elimination pathways of HA in est 25 shumans for the or and the

Figure 14 shows increased uptake of 5-FU in the stomach, brain and lungs.

Figure 15 shows the effect of HA on the pharmacokinetics elimination of plasma 5-FU.

. 6 belisded Figure 16 shows the criteria for definition of experimental end-point. Criteria 2 (Panel A) and Criteria 3 (Panel B) are shown.

Figure 17 shows the efficacy of 5-FU/HA adjuvant 10 therapy (6 week treatment regimen): Effect on primary tumour volume.

Figure 18 shows the efficacy of 5-FU/HA adjuvant therapy (6 week treatment regimen): Effect on body mass.

Figure 19 shows the efficacy of 5-FU/HA adjuvant therapy (6 week treatment regimen): Effect on spread of cancer lymph nodes and formation of new tumours.

Figure 20 shows the general appearance of tumours of the 6 month efficacy study.

Figure 21 shows the effect of HA/5-FU adjuvant therapy on patient survival.

Figure 22 shows the % change in body mass in mice treated with CMF/HA therapy over a 6-week period.

Figure 23 shows the % change in tumour volume in mice treated with CMF/HA therapy over a 6-week period.

Figure 24 shows the  $^{1}\mathrm{H}$  NMR spectrum of the MTX dissolved in  $H_2O$ . This spectrum readily identifies each group of hydrogens in the MTX.

Figure 25 shows the possible interactions of MTX 30 with HA.

Figure 26 shows the 600 MHz spectrum of hyaluronic acid at 600 MHz and 298 K.

Figure 27 shows the 600 MHz <sup>1</sup>H NMR spectrum of MTX alone and MTX with increasing additions of HA (50 kDa) of 2 nmoles, 10 nmoles, 20 nmoles and 80 nmoles at 298 K.

Figure 28 shows the 600 MHz  $^1\mathrm{H}$  NMR spectra of 5-FU and 5-FU (1.25 mg/mL, 1.6 mg/mL and 6.4 mg/mL) with HA

(750 kDa, 3 mg/mL) between 70.0 and 8.5 ppm, at 298 K.

	ABBREVIA	PIONS 1 20 LOSECTORES 1973
	BSA	Bovine serum albumin
5	Ci	Curies TARVANT THE TO MONTENING COLLEGES
• •	CMF	Cyclophosphamide, Methotrexate and 5-Fluorouacil
	Сус	Cyclophosphamide
	DNA	Deoxyribonucleic acid
	Dpm	Deteriorations per minute
10	DTTP	Deoxythymidine triphosphate
	ECM	Extracellular matrix
60 10	EDTA	Ethylenediaminetetraacetic acid
(d[	ELISA	Enzyme linked immunosorbent assay
	FCS	Foetal calf serum
<b>1</b> 5	5-FU	5-fluorouracil
w W	GAG	Glycosaminoglycan
<b>0</b>	GlcNAc	N-acetyl glucosamine
[15] [15] [15] [15] [15] [15] [15] [15]	GlcUA	Glucuronic acid
	HA	Hyaluronan/Hyaluronic acid
<b>2</b> 0	HABP	Hyaluronan binding protein
	HAase	Hyaluronidase
	HBSS	Hanks balanced salt solution
	HRP	Horse radical peroxidase
	h	hour
25	$K_{av}$	available volume of distribution within the gel
	1	Litre
30	min	minute
	PBS	Phosphate buffered saline
	PM	Plasma membrane
	RHAMM	Receptor for HA-mediated motility
	RMCa	Rat mammary carcinoma
	RNA	Ribonucleic acid
	RT	Room temperature
	S-phase	Synthesis phase
35	S.D.	Standard deviation
	SEM	Standard error of the mean
	$V_{e}$	volume of elution

52 1 3.1 C.

V<sub>o</sub> void volume

V<sub>t</sub> :: 3 oftotal volume

TGD Tumour growth delay

TDT Tumour Doubling Ti

5

10

15

COMPONIUM TOWNS

30

35

# DETAILED DESCRIPTION OF THE INVENTION

way of reference only to the following non-limiting examples. It should be understood, however, that the examples following are illustrative only, and should not be taken in any way as a restriction on the generality of the invention described above. In particular, while the invention is described in detail in relation to cancer, it will be clearly understood that the findings herein are not limited to treatment of cancer. For example, cytotoxic agents may be used for treatment of other conditions; methotrexate is widely used for treatment of severe rheumatoid arthritis.

20 Example 1

# Validation Of Human Breast Cancer Tumours In Nude Mice And Identification Of Hyaluronan Receptors On The Breast Tumours In Situ

Edvis & Fairtia

To establish an appropriate animal model for human breast cancer, it was necessary to perform pathological testing. For a tumour to be physiologically viable neovascularization is essential, because the capillary network supplies nutrients to the tumour. The presence of vascularisation, ductal invasion, necrosis, apoptosis, a high mitotic index and nuclear abnormalities are all characteristic of breast carcinoma.

The human breast carcinoma cell line MDA-MB-468 (American Tissue Culture Collection, Rockville, U.S.A) was selected on the basis of its expression of the HA receptors, CD44, RHAMM and ICAM-1. Cells were routinely grown and subcultured as a monolayer in 175cm<sup>2</sup> culture flasks in Leibovitz L-15 Medium supplemented with 10% foetal calf serum (FCS) and 10µg/ml gentamicin. For

15

20

25

35

1

injection into mice cells were grown to 100% confluency, trypsinised in 0.05% trypsin/0.01% EDTA solution, washed twice by centrifugation in a Beckman TJ-6 bench centrifuge (Beckman, Australia) at 400gav for 10min, counted using a 5 Model-ZM Coulter counter (Coulter Electronics, England), and resuspended in Serum-free Leibovitz L-15 medium at 1 x 108 cell/ml.

85 athymic Balb/c/WEHI nude female mice (Walter and Eliza Hall Institute of Medical Research, Melbourne, Australia), 6 to 8 weeks old, were maintained under specific pathogen-free conditions, with sterilised food and water available ad libitum. Ten million MDA-MB 468 cells were prepared as described above, and directly injected into the fat pad under the nipple of each mouse. Tumour growth was observed in 96% of mice. When the tumour growth was visually detectable, the tumour progression was monitored by weekly measurements of the tumour volume. Tumour volumes were calculated from 3 perpendicular diameters using the equation;

### $V=(1/6)p(d_1d_2d_3)$

where: V is tumour volume (in mm<sup>3</sup>),

d1 is the first diameter of the tumour (in mm),
d2 is the second diameter of the tumour (in mm),

and

d<sub>3</sub> is the third diameter of the tumour (in mm) (Lamszus et al, 1997).

30 Eight weeks after tumour inoculation the mean tumour size was  $482.2 \text{ mm}^3$  (SEM,  $39.8 \text{ mm}^3$ ).

Approximately 8 weeks after tumour induction two tumour-bearing mice were given a lethal dose of Nembutal. Within 3min of killing the mice, tumours were surgically removed and immediately fixed in 10% buffered formalin for 12 hours. The fixed tumour was dehydrated overnight in a series of 70-100% ethanol washes, followed by paraffin

15

20

25

30

embedding from which 2-4µm sections were cut. The sections were placed on slides, dewaxed, and brought to water. Slides were washed 3x5min in phosphate-buffered saline (PBS). Heterophile proteins were blocked by incubation with 10% foetal calf serum for 10min, followed by a PBS The detection antibodies were applied for 60min at room temperature (RT). The antisera or antibodies were directed against RHAMM (Applied Bioligands Corporation (Manitoba, Canada), ICAM-1, CD44v6, CD44v10, total CD44H, and CAE. All other detection antibodies were purchased from Zymed (California, U.S.A). The slides were washed 3x5min in PBS and endogenous peroxidase activity blocked by immersion in 0.3%H2O2/ methanol for 20min. further PBS wash, peroxidase-conjugated pig anti-rabbit secondary antiserum (Dako, Denmark) was applied for 60min at RT, followed by 3x5min wash in PBS. Sigma Fast DAB (3,3'-Diaminobenzidine, Sigma, St. Louis, U.S.A) tablets were prepared according to the manufacturer's instructions and the DAB solution was applied for 5-10min at RT. slides were washed in tap water for 10min, counterstained

with haematoxylin, dehydrated and mounted.

Examination of the haematoxylin and eosin-stained breast tumour sections demonstrated all of the usual features associated with viable tumours, as shown in Figures 3 and 4, confirming that the animal host successfully maintained a grade II human breast consistence.

- Figures 3 and 4, confirming that the animal host successfully maintained a grade II human breast carcinoma. There are several features which are characteristic of malignancy. The section of the slides labelled (B) displays these features. All of the pathological features of malignancy observed are in section (B), ie
  - i) high nuclear/cytoplasmic ratios
  - ii) angular chromatin and nucleoli
  - iii) irregular nuclear membrane

It was concluded that a grade II-III level tumour was capable of being supported in the nude mouse model. A grade II-III level tumour generally gives a prognostic survival rate of about 47% (Bloom and Richardson, 1957). A

ASSESSMENT OF THE PARTY OF THE

5

• .

10

₫ 15

,-⊒

20

description beautiful best of the additional grade II-III level tumour is characterised by:

- moderate nuclear pleomorphism, hyperchromatin, and mitotic activity, features observed throughout the displayed section of tumour; and
- little or no duct formation. ii) Large areas of necrosis (N) can be correlated with the tumour spread, which suggests a more aggressive invasive course (Carter, 1990). The infiltrating edge of the tumour is indicated by ( ).

A major aim of this experiment was validation that the histological and cytological behaviour of the tumours established in these mice were comparable to those of such tumours in their natural human hosts. In achieving this aim we have also shown that the tumour cells in the mice are of human origin and that they express highly relevant HA receptors such as RHAMM, CD44 and putative ICAM-1. Since it was hypothesised that tumour targeting could occur via receptor-mediated internalisation or binding, it was necessary to confirm the expression of HA receptors, ICAM-1, CD44 and RHAMM. Figures 5B-D demonstrates that all these receptors were present. 1 lists the degree of receptor expression on the two tumours tested.

# Table 1: Expression Of Hyaluronan Receptors On Human Breast Tumour Xenografts:

The rating index for the percentage of epitope expression

on the tumour was quantitated as:

21 le or no draw formation. - 80

1-25% in the first formula of instance (F) we impose the second of th

26-50% to ++tan open announcement of the control

THAT I TO BE THE SAME.

51-75% +++

10 76-100% ++++

5

HA receptor	Function .	Distribution on tumour	% epitope
			expression
CD44H	Isoform which	To-mark the state of the state	on tumour
	predominantly binds and internalises HA (Culty et al., 1992)	Expressed on all cells with exception of some stromal cells	++++
CD44v6	Role in cancer unknown,		
CD44V0	but is often used as a prognostic factor. The		+ .
	higher the expression,		
	the lower the survival		
	probability (Friedrichs		
	et al., 1995)		
CD44v3	Often over-expressed in		
	breast carcinoma		<u>-</u> -
	(Friedrichs et al., 1995)		
RHAMM	Required for	Groups of infiltrating	
". ·	transformation and tumour	tumour cells, with high	
٠	cell invasion (Hall et	expression on cells	+++
	al., 1995)	surrounding necrotic	
70111		areas	<u> </u>
ICAM-1	Binds and internalises  HA, putative metabolic receptor (McCourt et al., 1994)	Present on stromal cells	++
CEA	A fetal antigen expressed on malignant cells (Haskell, 1990)	Present on all tumour cells	++++

. . . . .

10

15

20

25

30

35

ed the spanish The human origin of the tumour cells was confirmed by staining the tumour and surrounding tissue with a human-specific cancer marker. The presence of CEA clearly demonstrated that the tumour was human, while being 5 maintained by the cardiovascular system of the murine host (Figure 5A). The polyclonal CEA antisera was selected, since it reacts exclusively with human CEA. This micrograph demonstrates that the tumour was entirely of human origin (H), as shown by the brown staining. surrounding tumour capsule and adipose tissue is definitely of mouse origin, as indicated by the lack of staining with the antisera (M). The brown staining demonstrates the high expression of RHAMM on the tumour cells. The greatest intensity of staining can be noted on the areas surrounding tissue necrosis and tumour infiltration.

### Preparation And Injection Of Methotrexate/ Example 2 Hyaluronan Drug Combinations

Having established the usefulness of the nude mouse model, it could now be used to test the effectiveness of a HA/MTX preparation.

A stock solution of MTX was prepared by dissolving powdered MTX in 0.5%w/v sodium carbonate (pH 9), and brought to a concentration of 24.5mg/ml with 0.9%w/v The stock solution was filtered through a 0.22µm filter to ensure sterility before addition of [3H]methotrexate and dilution to injection concentration with injection-grade sodium chloride. Comparative data on the pharmacokinetics of MTX have already been published for the nude mouse and humans (Inaba et al, 1988), and were utilised in the design of this study, to simulate human therapeutic doses as closely as possible. Individual injections were prepared according to individual mouse body masses, with the aim of delivering 15mg/kg MTX in 50µl (equivalent to a human therapeutic dose of 0.42mg/kg for a mean body weight of 60kg; Inaba et al, 1988).

Desiccated HA (modal Mr 8.9x105k Da) was added to

30

35

. ...

a portion of the 24.5mg/ml MTX stock solution and dissolved overnight with vortexing, to give a final concentration of 21mg/ml. To ensure sterility gentamicin was added to a concentration of 50µg/ml and incubated overnight at 4°C.

5 Following the addition of [3H]methotrexate the HA/MTX stock mixture was diluted to injection concentration with injection grade sodium chloride. Injections were individually made according to mouse body masses, to deliver 15mg/kg MTX and 12.5mg/kg HA in 50µl. With this quantity of HA injected into the body, saturation kinetics.

quantity of HA injected into the body, saturation kinetics would be observed for the period of the experiment (Fraser et al, 1983).

To ensure that the HA had maintained its molecular weight during the preparation of the

15 methotrexate/HA injection mixture, the injection solution was analysed on a Sephacryl S-1000 size exclusion gel (Pharmacia, Uppsala, Sweden) with column specifications of 1.6cm x 70cm, sample size 2ml, flow rate 18ml/h and 2ml fraction size. Figure 6 shows that HA retained its

20 molecular weight during the mixing procedure.

Mice were randomly divided into 2 groups of 40 animals. Group I received MTX only, and Group 2 received MTX/HA combination therapy. Animals were individually placed in an injection box, and the injections were administered via the tail vein. Tritiated methotrexate (mean injected disintegration's per minute (dpm) ± standard error of the mean (SEM): 19,159,146 ± 1,336,819) contained within 15mg/kg MTX ± 12.5mg/kg HA was delivered in each injection. Mice were individually housed in soft, non-wettable plastic enclosures so urine could be collected. At 30min, 1h, 2h, 4h or 8h after injection mice were

At 30min, 1h, 2h, 4h or 8h after injection mice were anaesthetised by 0.1ml intra-peritoneal injection of Nembutal (Glaxo, Australia Pty. Ltd., Melbourne, Australia), and blood was collected from the heart or great vessels using a needle and syringe. After blood collection the animals were killed by cervical dislocation.

Blood was delivered into EDTA-coated glass tubes

20

30

and plasma was prepared by centrifugation at 14,000gav for 10min. Radioactivity was counted in 50µl aliquot's after decolourisation with 100µl of 30%v/v hydrogen peroxide and the addition of 3ml HiSafeII scintillant. To overcome chemi- and photoluminescence, samples were counted for 2min in a Wallac 1410 ß-counter over a 3, 7 or 20 d period, depending on the sample source. During the periods between counting, samples were stored in the dark at ambient temperature. All calculations were performed on stabilised samples from which all chemi- and photoluminescence had been removed.

To determine the percentage of injected MTX in the plasma, it was necessary to calculate the total plasma volume of each mouse (ml), using the standard formula:

Mouse mass (g) x mouse blood volume (0.07) x plasma proportion of blood (0.59)

The percentage of injected MTX in the plasma was then calculated:

# Plasma volume (ml) x dpm/ml plasma x 100 total dpm injected

25 = % injected MTX in plasma.

To ensure an accurate quantitation of the amount of MTX delivered to the blood stream, the injection site on the tail vein was dissected and the MTX quantitated. The mean percentage of the MTX injection remaining at the injection site was 3.78% (SEM: 0.57%). The amount of MTX delivered to the bloodstream (MTX available for distribution to the tissues and tumour) was calculated as:

Amount of MTX Difference in Dpm/mg of Dpm remaining

35 delivered to = mass of injection X injection - at injection
bloodstream syringe (mg) material site

(Dpm)

The amount of MTX delivered to the bloodstream henceforth will be referred to as the "injected dose".

In order to make accurate comparisons between the sample population and normalise slight variations in organ and tumour masses, the concentration of MTX in the body organs and tumour and body fluid was expressed as % of injected dose/gram of tissue.

The mean percentage of the MTX injection

remaining at the injection site was 3.78% (SEM: 0.57%). To normalise such variations, the percentage of dpm found in tumour and tissues was calculated as a percentage of the dpm injected minus the dpm found remaining at the injection site. This amount is henceforth referred to as the

available dpm or available methotrexate. The results are summarised in Table 2.

# oomsoro, owlyor

Table 2: Methotrexate uptake in mouse tumours, organs and body fluids

Values are the median + SEM, where n=8

# represents MTX Dpm in total plasma volume of mouse. Figures represent Plasma MTX Dpm as % if the injected MTX dose 🕈 and 🗀 🕮 represent statistically significant figures when data is analysed using the Manu-Whitney Rank Sum Test @ represents MTX Dpm in total urine of mouse. Figures represent as % of the injected dose. N=3-8 ID represents insufficient data for analysis

								,		• • • • • • • • • • • • • • • • • • • •
		MTX only	nly	(median %±SE)		WHANTX (medjan%±SE)	HAM	LX.	(median?	é±SE)
	30 min	1 Hr	2 Hr	4 Hr	4 Hr % 新8 Hriti 30 min	30 min	1 Ar	2 Hr	4Hr 28 Hr	28 Hr
Tumour	0.66±0.09		0.50+0.045 [0.32+0.03]	1 1	0.31±0.02 (012±0.05) 0.88±0.04[0362±0.03* 0.48±0.32*	0.88+0.04	0.62±0.03*	0.4640,32*	0.34±0.12   0.17±0.02	0.17+0.02
Liver	9,56±1.92	4.63±1.50	2.13±0.55	$2.11\pm 2.16$	2.11±2.16   0771±1184   12.83至166 7.14±0.92 2.43+0.24	12.83+1.66	7.14±0.92	2.43+0.24	1.99+0.45	1.99+0.45 0.49+0.08
Spleen	0,39±0.09	0.24±0.18	0.17±0.05	0.26±0.05	0.26+0.05 0112+0.01 0.48+0.06	0.48+0.06	0.34+0.03	0.24+0.03		0.14+0.00
Lymph Nodes	2.33±0.39	0.89±0.55	0.69+0.42	0.94,10.19	0.94±0.19 16,26±0.08, 1.28±0.23	1.28+0.23	1	1.49+0.26 0.58+0.10 0.24+0.08 0.10+0.01	0.24+0.08	0.10+0 01
Left Kidney	0.41±0.05	0.13±0.02	0.08±0.01	0.13+0.03	0.13±0.03 (0;04±0:00 0.39±0.04	0.39+0.04	1	0.16±0.05 0.09±0.00 0.10±0.04 0.04±0.02	0.10+0.04	0,04+0.02
Right Kidney	0.40±0.06	0.14±0.01	0.10±0.02	0.11+0.01	0.11±0.01   0.04±0.00   0.46±0.06	0.46±0.06		0.10±0.01	0.08+0.05 0.05+0.01	0.05+0.01
Bladder	8.44±39.0.	5.46±5.30	1.65±1.08	1.63+1.49	1.63±1.49   0:50±0:66   5.29±16.07   16.96±8.99	5.29±16.07	16.96+8.99	3.18+3.89	3.18+3.89 1.89+3.16 0.21+0.04	0.21+0.04
Intestines	11.75±2.26	16.89±8.51	10.41±2.59	10.83+3.04	10.83±3.04 3,38±1,68 5,65±1,75	5.65+1.75	9.66+5.73	5.84+4.16	5.84+4.16   4.55+2.64   1-12+1 71	1-12-1171
Stomach	3.75±2.10	4.38±1.73	5.86±1.22	0.84+0.31	0.84+0.31 (0.24+0.06 2.64+0.68)	2.64+0.68		4.52+0.59	1 24+0 71-10 40+0 20	0 40+0 20
Brain	0.13±0.03	0.10±0.03	0.08+0.12	0.14+0.03	0.14+0.03 (0.08+0.00) 0.17+0.02	0.17+0.02		0.10+0.02		0.040.01
Heart	0.44±0.03	0.37±0.13	0.20±0.24	0.21+0.03	0.21±0.03 (0.10±0.03 0.53±0.05	0.53+0.05	0.26+0.04	0.16+0.04	0.16+0.04   0.16+0.09   0.12+0.01	0 12+0 01
Lungs	0.90±0.11	0.40±0.14	0.30±0.16	0.33 +0.07*	0.33±0.07* 0.15±0.14 1.03±0.12	1.03+0.12		0.24+0.09	0.24+0.09 0.16+0.01 0.14+0.02	0 14+0 02
Uterus	0.67±0.12	0.33±0.23	0.30+0.07	0.2710.07	0.27±0.07   0.113±0.01   0.78±0.70   0.62±0.24	0.78+0.70	0.62+0.24	0.28+0.12	0.28+0.12 0.19+0.14	111001
Plasma#	1,49±0.31	1.51±0.48	0.45±0.23	0.31+0.12	0.31±0.12   0115±0.02   1.06±0.28   0.53+0.34	1.06+0.28	0.53+0.34	0.31+0.15	0.31+0.15 0.42+0.15 0.13+0.00	0 1340 00
Urine@	14,28±1.65	9.06±3.47%	20.44±3.38	23.55±4.01	23.55±4.01   初初の   15.64±4.46   18.03±2.44   12.81±2.41   35.58±6.05   15.	15.64+4.46	18,03±2,44	12.81+2.41	35.58+6.05	20.71

15

25

30

35

No statistically significant difference was noted in the plasma levels of MTX when the drug was co-injected with HA. The gross pharmacokinetics of MTX remained unaltered, with maximum MTX plasma levels reached within 0.5 to 2h following intravenous administration (MIMS, 1997):

When possible urine was collected from the non-wettable plastic enclosures with a syringe and needle. The urine was cleared by centrifugation at 14,000gav for 10 min. Its radioactive content was measured after the addition of 3ml HiSafeII scintillant to samples ranging from 8-30µl. Despite the technical difficulties in accurately quantitating the volume of urine produced by each mouse we calculated the percentage of injected MTX dose in the urine by the following formula:

# time of collection (h) x $42\mu$ l x dpm/ $\mu$ l urine x 100 Total dpm injected

20 = % of injected MTX in urine.

It was not possible to collect urine from each mouse, because of variations in the micturition rate. When 3 or more urine specimens were available per time point per treatment non-parametric statistical analysis of the data at those time points was performed. At one hour after administration there was 50% (p=0.043) more MTX in the urine of mice which received MTX/HA (see Table 2).

Immediately after killing the mouse the tumour, liver, heart, spleen, bladder, left and right kidneys, uterus, lungs, stomach, intestines, brain and lymph nodes were excised and analysed for total radioactivity. The total radioactivity in each tissue was determined by solubilising 100-400mg of tissue in 3-6ml of OptiSolv (ACC, Melbourne, Australia) for 36 h, 22°C. On completion of solubilisation, radioactivity in the tissue was counted after adding 10ml of HiSafeIII scintillant. Again to overcome chemi- and photoluminescence, samples were counted

for 2min in a Wallac 1410 ß-counter over a 3, 7 or 20 d period depending on the sample source. During the periods between counting, samples were stored in the dark at ambient temperature. All calculations were performed on stabilised samples from which all chemi- and photoluminescence had been removed. Figures represent median ± SEM (n=8).

It was important to establish that metabolically active organs such as the liver, spleen and kidneys did not experience a high level of drug targeting which could counter-act any positive aspects of increased tumour targeting. Table 2 lists the methotrexate uptake of each tissue at the various time points tested.

10

15

20

25

30

35

Utilising the Mann-Whitney Rank Sum Test and Students t-test there was no statistically significant difference in MTX concentration/g tissue when MTX was coinjected with HA. Because of the small number of animals at each time point, the Mann-Whitney test became statistically invalid if one data point overlapped, but in the liver, uterus and intestine a definite trend could be observed.

In the liver there appeared to be a short-term increase in the uptake of MTX when it was combined with HA, as shown in Figure 7.

At 30min and 1h the liver contained a median increase in MTX concentration of 65% and 26% respectively. At 2h no difference was observed in the amount of MTX in the liver regardless of treatment. An interesting trend became apparent after 4h, when less MTX was found in the liver when it was co-injected with HA (4h: 68% less MTX and 8h: 75% less MTX), as shown in Figure 8.

There was a significant trend in the intestine, where the combination of HA and MTX resulted in a decreased uptake of the drug at every time point, as shown in Figure 9.

The intestine was fully homogenised, followed by solubilisation of approximately 400mg of tissue in 3-6ml of

\*

OptiSolv for 24h at 22°C, followed by the addition of 10ml Hisafe-3 scintillant. To overcome chemi- and photoluminescence, samples were counted for 2min in a Wallac 1410 ß-counter over a 3, 7 or 20 d period depending on the sample source. During the periods between counting, samples were stored in the dark at ambient temperature. All calculations were performed on stabilised samples where all chemi- and photoluminescence had been removed.

The figures represent median  $\pm$  SEM (n=8).

Analysing the data with the non-parametric randomization test for matched pairs demonstrated that the coadministration of HA significantly reduced the excretion of drug into the GI tract (p=0.031, one-tailed test).

The decrease in MTX concentration ranged from 43-67%. The non-parametric randomization test for matched pairs showed that the co-administration of HA significantly reduced the excretion of drug into the gastrointestinal tract (p=0.031, one-tailed test).

In the lungs there was significantly less MTX present at 4h when co-administered with HA, with a median decrease of 52% (p=0.014). No differences were demonstrated at other time points, however, so that the significance of this observation remains uncertain.

No observable trends were detected in the spleen, uterus, brain, heart, lymph nodes, stomach and kidneys.

There are two possible mechanisms of HA targeting of methotrexate to tumour cells (Figure 10).

There was a significant targeting effect when HA was combined with MTX (Figure 7). The greatest relative increase in tumour retention of drug was observed at 0.5h (mean 24% increase), 1h (mean 30% increase) and 2h (mean 119% increase), whereas at 4h and 8h the increase was negligible. Because of the small population size and non-parametric distribution of the data the Mann-Whitney Rank Sum Test test was used, and revealed a significant increase in tumour uptake of drug when HA was co-injected. At 1h the statistical significance was p=0.021 and at 2h,

10

□ □ □

Ų

20.

25

30

35

p=0.050. The other time points did not demonstrate a statistically significant difference, but the trend in MTX concentration/g of tumour was consistently greater when coinjected with HA.

The data shown in Figure 7 unequivocally demonstrate that co-administration with HA has greatly increased the uptake of MTX by the tumour within 30min after injection. Moreover, co-administration also sustains a distinctly higher level during the subsequent decay in the concentration of drug within the tumour. At 1h the difference was significant at p=0.021 ( $n_1$  =8,  $n_2$  =8), and at 2h when p=0.05 ( $n_1$  =8,  $n_2$  =8) as assessed by non-parametric tests.

HA containing entrapped MTX binds to the receptors (CD44 and/or I-CAM-1) and is internalised via receptor-mediated endocytosis, so releasing the drug into the tumour cell.

The HA molecular mesh will act as an impediment to outward diffusion, so that after HA binds to receptors (CD 44, RHAMM and/or ICAM-1), the entrained MTX is able to diffuse into the tumour cells. While held at the surface of the cells by the HA matrix the MTX has increased availability to the active transport mechanism normally utilised for MTX transport into the underlying cell.

The side-effects and the distribution of a drug to tissues other than the desired sites of activity can also be influenced by its association with HA. For example, HA is normally cleared from the bloodstream by receptor-mediated cellular uptake and catabolism in the liver (80-90%), kidneys (10%), spleen and bone marrow, with some minor species variation in the last two sites. As expected HA does seem to increase hepatic delivery of the drug at least for a short time. At 30min and 1h the liver showed a median increase in MTX concentration of 65% and 26% respectively. At 2h no difference was observed in the amount of MTX in the liver, regardless of treatment. An interesting trend became apparent after 4h, where less MTX

10

15

20

25

30

35

was found in the liver when it was co-injected with HA (4h: 68% less MTX and 8h: 75% less MTX). After intravenous administration MTX is widely distributed in body water, and can be retained in the liver for months (McEvoy, 1988); therefore the decreased median concentration of MTX in the 5 liver at 4 and 8h when co-injected with HA could indicate an altered balance in the routes of pharmacokinetic clearance. Considering that HA is rapidly metabolised within the liver endothelial cells (LEC) it follows that MTX which is co-internalised with HA would be released within the liver sinusoidal lining cells, where it could either diffuse into hepatocytes to be secreted in the bile and subsequently the gastrointestinal tract, or be returned to the circulation for further distribution into body water and for urinary excretion, or both.

There could be a therapeutic advantage of short-term hepatic-targeting. In the case of liver metastasis a rapid, high exposure to MTX could be beneficial, and since the observed targeting is only for 1h this would counteract any long term toxicity problems. Liver targeting could be utilised with drugs which require bio-activation, eg mitomycin C, doxorubicin, where the drug/HA mixture would be targeted to the LEC. With the inactive drug concentrated in the LEC it would be able to diffuse into the hepatocytes for activation, thus acting as an activation targeting mechanism.

One of the major sites of toxicity of MTX is the gastrointestinal tract. Co-administration of MTX with HA significantly diminished the amount of drug delivered to the GI tract. There may be several mechanisms associated with the decreased concentration of MTX in the gut.

Methotrexate is a very small molecule, which one would expect normally to pass through most capillary walls, whereas association with HA would greatly reduce its passage through this route.

Rapid degradation of HA in the liver endothelial cells resulted in a rapid release of MTX into the liver and

return to the bloodstream, where it would undergo increased renal clearance, as indicated at 1h, and which 50% more MTX was excreted in the urine of mice receiving MTX/HA preparations.

The main pathway for the final elimination of MTX from the body is urinary excretion. There seems to be little increase in renal content of the drug with HA, but we believe from other evidence that HA is taken up and catabolised very quickly by the kidneys, so that its residence time would be short and associated drug would be quickly released into the urine.

### Conclusion

10

15

25

30

35

OPEGET, CELEBRO

The results reported here represent the first stage of a pre-clinical study to examine the proposition that administration of therapeutic agents together with hyaluronan will achieve their selective delivery to the desired target of pathological tissue; thus achieving a higher and more effective concentration at that point. In this case methotrexate, a cytotoxic drug widely used in current treatment regimens for human mammary cancer and other human malignancies, and for rheumatoid arthritis, has been studied by the intravenous route of administration with and without hyaluronan.

We have found that the nude mouse model is a particularly suitable model for the study of human breast cancer in a living host, and to resolve some fundamental matters in the use of HA to direct therapeutic agents to the sites of diseased tissue, and thus to enhance their beneficial effects. Our results have been achieved with a drug of small molecular weight that shows no specific form of association with HA, demonstrating that HA can still deliver such a drug in enhanced amounts to pathological tissue when injected into the bloodstream. This study demonstrates that in the conditions prevailing in the body, the MTX is sufficiently retained with HA to effect a significant enhancement of delivery to human breast cancer,

15

20

25

al 1993).

as well as potentially reducing the undesired side-effect of gastrointestinal toxicity. - - 23 3 2 CM

### Example 3 Preparation And Injection Of Paclitaxel/ Hyaluronan Drug Combinations

Built of the cream to Having established the usefulness of the nude mouse model for HA/Paclitaxel, it could now be used to test the effectiveness of other chemotherapeutics. It was decided that, due to its therapeutic importance, paclitaxel (also known as taxol) would be used.

Paclitaxel is isolated from the Western Yew, Taxus brevifolia, (Wani et al 1971), and is clinically active against advanced ovarian and breast cancer (Rownisky et al 1990; McGuire et al 1989) and is currently undergoing clinical trials for treatment of a variety of other cancers. However the main problem associated with paclitaxel is its extreme lipophilicity and consequent poor aqueous solubility. Efforts to solve this problem have led to the synthesis of paclitaxel analogues and prodrugs along with extensive efforts to devise safe and biocompatible formulations. To date no prodrugs have shown sufficient stability, solubility or activity that would warrant clinical development (Mathew et al 1992; Vyas et al 1993). However, semisynthetic taxanes are showing greater solubility and potency than paclitaxel (Bissery et al 1991) and one form Taxotere has entered human trials (Bisset et

The current clinical formulation of paclitaxel employed for intravenous delivery utilises ethanol and 30 Cremophor EL in a 1:1 (v/v) ratio with the drug at 6 mg/mL. Cremophor EL is actually polyethoxylated castor oil; a clear, oily viscous, yellow surfactant. Stability studies have shown that the original formulation has a shelf-life of 5 years at 4°C. The preparation is diluted before use 35 with 0.9% saline or 5% dextrose to concentrations of 0.3-1.2 mg/mL and the physical and chemical stability of the material in these conditions is ca. 27 h.

15

20

25

30

35

dilution of the vehicle to these levels can produce a supersaturated solution (Adams et al 1993) that may be prone to precipitation if used outside the established guidelines. Therefore an in-line filter is required during administration as a safeguard against the infusion of particulates. It is also recommended that diluted paclitaxel solutions be used within 24 h of preparation. Hazing of the above solutions has also been observed and has been attributed to the extraction of plasticisers by Cremophor from the infusion bags and tubing (Waugh et al 1991).

In addition to the problems of physical instability mentioned previously the most significant problem with Cremophor is the fact that it is reported to have pharmacological activity. A variety of drugs are administered using Cremophor EL including cyclosporin, tacrolymus and teniposide. However, the dose of Cremophor EL given with paclitaxel is higher than with any other marketed drug. Cremophor has been observed to cause serious or fatal hypersensitivity episodes. Vehicle toxicity may also be largely responsible for fatal or life threatening anaphylactic reactions observed upon rapid infusion of paclitaxel into animals or humans (Dye & Watkins 1980; Lorenz et al 1977; Weiss et al 1990).

A stock solution of paclitaxel is prepared by and individual injections are prepared according to individual mouse body masses.

Desiccated HA (modal Mr 8.9x10<sup>5</sup>k Da) is added to a portion of the 24.5mg/ml paclitaxel stock solution and dissolved overnight with vortexing, to give a final concentration of 21mg/ml. To ensure sterility gentamicin is added to a concentration of 50µg/ml and incubated overnight at 4°C. Following the addition of [<sup>3</sup>H]paclitaxel the HA/paclitaxel stock mixture is diluted to injection concentration with injection grade sodium chloride. Injections are individually made according to mouse body masses, to deliver 15mg/kg paclitaxel and 12.5mg/kg HA in

20

25

50µl. With this quantity of HA injected into the body, saturation kinetics would be observed for the period of the experiment (Fraser et al, 1983).

To ensure that the HA had maintained its

molecular weight during the preparation of the
paclitaxel/HA injection mixture, the injection solution is
analysed on a Sephacryl S-1000 size exclusion gel
(Pharmacia, Uppsala, Sweden) with column specifications of
1.6cm x 70cm, sample size 2ml, flow rate 18ml/h and 2ml
fraction size. Figure 4 shows that HA retained its
molecular weight during the mixing procedure.

Mice are randomly divided into 2 groups of 40 Group I received paclitaxel only, and Group 2 animals. receive paclitaxel/HA combination therapy. Animals are individually placed in an injection box, and the injections are administered via the tail vein. Tritiated paclitaxel (mean injected disintegration's per minute (dpm) ± standard error of the mean (SEM): 19,159,146 ± 1,336,819) is delivered in each injection. Mice are individually housed in soft, non-wettable plastic enclosures so urine can be collected. At 30min, 1h, 2h, 4h or 8h after injection mice are anaesthetised by 0.1ml intra-peritoneal injection of Nembutal (Glaxo, Australia Pty. Ltd., Melbourne, Australia), and blood is collected from the heart or great vessels using a needle and syringe. After blood collection the animals are killed by cervical dislocation.

Blood is delivered into EDTA-coated glass tubes and plasma is prepared by centrifugation at 14,000gav for 10 min. Radioactivity is counted in 50µl aliquots after decolourisation with 100µl of 30%v/v hydrogen peroxide and the addition of 3ml HiSafeII scintillant. To overcome chemi- and photoluminescence, samples are counted for 2min in a Wallac 1410 ß-counter over a 3, 7 or 20 d period, depending on the sample source. During the periods between counting, samples are stored in the dark at ambient temperature. All calculations are performed on stabilised samples from which all chemi- and photoluminescence had

WO 00/41730

been removed.

CONTRACTOR OF THE STATE OF THE To determine the percentage of injected paclitaxel in the plasma, it is necessary to calculate the total plasma volume of each mouse (ml), using the standard formula: the second of the second of the second of

Mouse mass (g) x mouse blood volume (0.07) x plasma proportion of blood (0.59)

The percentage of injected paclitaxel in the plasma is then 10 calculated:

# Plasma volume (ml) x dpm/ml plasma x 100

total dpm injected

**15** 

5

= % injected paclitaxel in plasma.

To ensure an accurate quantitation of the amount of paclitaxel delivered to the blood stream, the injection site on the tail vein is dissected and the paclitaxel The mean percentage of the paclitaxel quantitated. injection remaining at the injection site is also determined. The amount of paclitaxel delivered to the bloodstream (paclitaxel available for distribution to the tissues and tumour) is calculated as:

25

ڄځ

u C

Dpm remaining Dpm/mg of Difference in Amount of paclitaxel injection - at injection = mass of injection Х delivered to site material bloodstream syringe (mg) (Dpm)

30

35

The amount of paclitaxel delivered to the bloodstream henceforth is referred to as the "injected dose".

In order to make accurate comparisons between the sample population and normalise slight variations in organ and tumour masses, the concentration of paclitaxel in the body organs and tumour and body fluid is expressed as % of injected dose/gram of tissue.

The mean percentage of the paclitaxel injection remaining at the injection site is calculated. To normalise such variations, the percentage of dpm found in tumour and tissues is calculated as a percentage of the dpm injected minus the dpm found remaining at the injection site. This amount is referred to as the available dpm or available paclitaxel.

When possible urine is collected from the non-wettable plastic enclosures with a syringe and needle. The urine is cleared by centrifugation at  $14,000g_{\rm av}$  for 10 min. Its radioactive content is measured after the addition of 3ml HiSafeII scintillant to samples ranging from  $8-30\mu l$ .

Immediately after killing the mouse the tumour, liver, heart, spleen, bladder, left and right kidneys, uterus, lungs, stomach, intestines, brain and lymph nodes are excised and analysed for total radioactivity. total radioactivity in each tissue is determined by solubilising 100-400mg of tissue in 3-6ml of OptiSolv (ACC, Melbourne, Australia) for 36 h, 22°C. On completion of solubilisation, radioactivity in the tissue is counted after adding 10ml of HiSafeIII scintillant. Again to overcome chemi- and photoluminescence, samples are counted for 2min in a Wallac 1410 ß-counter over a 3, 7 or 20 d period depending on the sample source. During the periods between counting, samples are stored in the dark at ambient temperature. All calculations are performed on stabilised samples from which all chemi- and photoluminescence had been removed.

# 30 Example 4 Use Of 5-Fluorouracil And HA Introduction

10

15

20

25

35

5-Fluorouracil is (5-FU) an antimetabolite that is commonly used in the treatment of breast and gastrointestinal tract cancers (Piper & Fox, 1982). 5-FU is converted to its active nucleotide form intracellularly where it interferes with both DNA and RNA synthesis. The drug functions via two mechanisms in vivo:

10

25

30

- (i) FdUMP binds tightly to thymidylate synthase preventing the formation of thymidylate, which is an essential precursor of deoxythymidine triphosphate (dTTP) which is one of the four deoxyribonucleotides required for DNA synthesis. The thymine-less state created by this inhibition is toxic to actively dividing cells (Pinedo & Peters, 1988).
- (ii) The second way in which 5-FU functions is that the incorporation of FUTP into RNA interferes with RNA function. The inhibition of thymidylate synthase caused by Fdurd and 5-FU incorporation into RNA is capable of causing cytotoxic effects on cells. Both the concentration and duration of exposure of 5-FU are important determinants of cytotoxicity. As RNA-directed effects are probably predominant with prolonged duration of exposure, where as DNA-directed effects might be more important during short-term exposure of cells in S phase.

Several studies have examined the use of HA as a drug delivery system for anti-cancer drugs. Coradini et al (1999) covalently bound sodium butyrate to HA, to determine whether this HA/sodium butyrate combination would enhance drug uptake by breast cancer cells in vitro. This study indicated that the mechanism of action of HA as a drug delivery vehicle may involve the HA-butyrate-ester derivative being carried to the CD44 receptors. HA/drug complex was internalised, followed by cytoplasmic hydrolysis of the HA/drug complex, subsequently releasing the butyrate which exerted an anti-proliferative effect. One in vivo study has been performed which covalently linked mitomycin C to HA as a means of treating murine Lewis lung xenografts (Akima et al, 1996). It was found that the HA-MMC complex resulted in anti-tumour activity at a low dose of 0.01mg/kg where the sole agent, mitomycin C did not demonstrate anti-tumour activity.

## Investigation Of The Synergistic Action Of Example 5 5-FU And HA In Human Breast Cancer Cells

Human breast adenocarcinoma cell lines MDA-MB-468, MDA-MB-435 and MDA-MB-231 were selected based on HA binding affinity (Culty et al. 1994) and the expression of the HA receptors of CD44 and RHAMM (Wang et al, 1996). Summaries of the cell line characteristics are shown in Table 3.

5

# edeaca cateda

10

Table 3: Hyaluronan Binding And Receptor Expression Of
Human Mammary Carcinoma Cell Lines

Cell Line	Type of breast	Degree of	HA Receptor	r
	cancer	HA Binding <sup>a</sup>	Expression	· · · · · · · · · · · · · · · · · · ·
			CD44	RHAMM
MDA-MB-231	adenocarcinoma	++	+++	+++
MDA-MB-468	adenocarcinoma	++++	++++	++
MDA-MB-435	ductal	+	+++	ND
	carcinoma	<u></u>		<u> </u>

a: Culty et al, 1994 b: Wang et al, 1996

Cell lines MDA-MB-468, MDA-MB-435 and MDA-MB-231 were routinely cultured as described in example 1.

It can be seen from Table 4 that breast cancer cells grown in media containing 0nM 5-FU + 100nm of HA did not demonstrate a statistically significant proliferative or cytotoxic effect when compared to untreated cells.

10

## Table 4: Effect Of Hyaluronan On Breast Cancer Cell Proliferation

Cell Line	0nM 5-FU	0nM 5-FU +100nM HA
	(mean cell number + 1	(mean cell number <u>+</u> 1
	s.D.)	S.D.)
MDA-MB-231	34,206 <u>+</u> 3,206	29,470 <u>+</u> 4,452
(n=4)		-
MDA-MB-468	36,751 <u>+</u> 2,814	37,607 <u>+</u> 3,325
(n=4)		
MDA-MB-435	117,760 ± 2,175	121,918 + 7,851
(n=4)		

Statistical testing was conducted using both the non-parametric Rank Sum Test and parametric Student's t-test

Therefore all results were expressed as a percentage of the 0nM 5-FU/0nM HA cell count. Distinct differences in growth patterns were noted between cell lines, for example MDA-MB-231 and MDA-MB-468 cells demonstrated a poor plating efficiency, where numerous floating cells were present before application of the test media. The MDA-MB-435 cell line demonstrated a high plating efficiency and a very rapid growth rate.

5

15

20

25

When HA was combined with 5-FU a syngeristic

10 cytotoxic effect was observed with the MDA-MB-468 cell
line, but not with the MDA-MB-231 or MDA-MB-435 breast
cancer cell lines. This is shown in Figure 11. The IC<sub>50</sub> of
5-FU alone was >50μm, but when combined with HA the IC<sub>50</sub> was
40nM, a reduction in drug dosage of up to 1250 times.

The results from the *in vitro* experiments demonstrated an increase in cell kill when 5-FU was applied to the breast cancer cells in the presence of HA. The MDA-MB-468 cells showed the greatest susceptibility to the 5-FU/HA therapy where the IC<sub>50</sub> was decreased from >50µM to 40nM, whereas both the MDA-MB-231 and MDA-MB-435 were not greatly affected by the 5-FU/HA combination. All of the breast cancer cell lines expressed high levels of the CD44 receptor with the MDA-MB-468 (60-80%), MDA-MB-231 (40-60%) and MDA-MB-435 (40-60%) as determined by Culty *et al* (1994). It has been demonstrated that the three cell lines used in these experiments are able to degrade HA, implying that the function of CD44 in tumour cells may be to mediate the degradation of HA (Culty *et al*, 1994).

Another factor to consider is the previous

exposure of the cells to chemotherapeutic drugs. Before a cancer cell line is isolated from a patient, the cancer sufferer has often undergone chemotherapy or radiation, which could result in the tumour containing treatment-resistant cells. In the case of MDA-MB-435 and MDA-MB-231, the patients from which the cell lines were derived had both been previously exposed to 5-FU (Cailleau et al, 1974). Since cancer cells contain several adaptation

10

15

20

30

35

mechanisms to overcome drug cytotoxicity, it is very likely that the tumour mass that remained after treatment was resistant to 5-FU, subsequently altering the susceptibility of the cells to the drug *in vitro*.

With the view of extrapolating any in vivo data obtained mice to the treatment of human counterparts, the experimental model and design was carefully developed. To definitively demonstrate the in vivo targeting and therapeutic efficacy of 5-FU/HA adjuvant therapy on human breast cancer xenografts, the following factors were examined:

Human breast cancer tumours were established in a well-validated Walter and Eliza Hall Institute strain of nude mouse, a widely accepted model for such studies which avoids an immune response against allogenic cells.

Comparative data on the pharmacokinetics of 5-FU that have already been published for the nude mouse and humans (Inaba et al, 1988), and were utilised in the design of this study, to simulate human therapeutic doses as closely as possible.

A major aim was validation that the histological and cytological behaviour of the tumours established in these mice were comparable to that of such tumours in their natural human hosts. In achieving this aim we have also shown that the tumour cells in the mice are of human origin and that they express highly relevant HA receptors such as RHAMM and CD44.

#### Example 6 Preparation Of HA And 5-FU Solutions

A stock of HA solution (10µM, 7mg/ml) was prepared by dissolving desiccated HA (modal  $M_{\rm r}$  7x10 $^5$ kDa,) in 0.9% w/v pyrogen-free injection grade NaCl. To ensure a homogenous solution the HA was dissolved overnight at  $4^{\circ}$ C followed by thorough vortexing. To ensure that the HA had maintained its molecular weight during the preparation of the stock solution, the solution was analysed on a Sephacryl S-1000 size exclusion gel with column

10

15

25

30

by the uronic acid assay.

specifications of 1.6cm  $\times$  70cm, sample size 2ml, flow rate 18ml/h and 2ml fraction size. The HA was used at a final concentration of 100nM, with all dilutions made in the appropriate growth medium.

The stock solution of 5-FU was prepared by dissolving 5-FU in 0.1M sodium hydroxide and brought to a concentration of 20mg/ml with 0.9%w/v pyrogen-free injection grade NaCl. The stock solution was filtered through a 0.22µm filter to ensure sterility before addition of [3H]-FU and dilution to injection concentration with injection grade sodium chloride. Individual injections were prepared according to individual mouse masses, with the aim of delivering 30mg/kg 5-FU in 50µl (equivalent to human therapeutic dose of 10.5mg/kg for a mean body weight of 60kg; Inaba et al, 1988). A pyrogen-free, HA stock solution (10mg/ml; modal  $M_{\rm r}$   $7 {\rm x} 10^5$  Da) was added to a portion of the 20mg/ml 5-FU stock solution and incubated overnight with vortexing, to a final HA concentration equivalent to 12.5mg/kg of mouse mass. Injections were 20 individually made according to mouse masses, to deliver 30mg/kg 5-FU and 12.5mg/kg HA in 50µl. With this quantity of HA injected into the body, saturation kinetics would be observed for the period of the experimentation (Fraser et To ensure that the HA had maintained its al, 1983). molecular weight during the preparation of the injection mixture, the injection solution was analysed on a Sephacryl S-1000 size exclusion gel with column specifications of 1.6cm x 70cm, sample size 2ml, flow rate 18ml/h and 2ml fraction size. Hyaluronan was detected in column fractions

The uronic acid assay was used to detect the presence of hyaluronan qualitatively from the fractions collected from the gel filtration chromatography procedure. A  $25\mu l$  aliquot of each fraction was then transferred into a 96 well plate. 250 $\mu$ l of a carbazole reagent (3M 35 carbazole/0.025M borate in  $H_2SO_4$  ) was then added to these fractions. The 96 well plate was incubated for 45-60min at

25

30

35

10

 $80^{\circ}$ C. A Dynatech MR7000 plate reader with a 550nm filter was used to read the 96 well plate. The absorbance was considered to be significant when it was >3 standard deviations above the background absorbance. The background was calculated by taking an equal number of sample points before and after  $V_o$  and  $V_t$  where the average number taken was 16 (Fraser et al. 1988).

The formulation of HA and 5-FU (10mg/ml HA and 20mg/ml 5-FU in 0.5% NaCl, pH 8.9) did not demonstrate a degradative effect on the molecular weight of the HA. Chromatographical analysis in a size exclusion gel indicated the maintenance of the modal molecular weight of 700,000Da.

15 Example 7 Drug Cytotoxicity Assay: Experimental Design

In designing drug titration experiments in vitro it is desirable to apply drug concentrations similar to the concentrations reached in plasma after intravenous administration. When 5-FU is therapeutically administered by an intravenous route (iv) at 10.5mg/kg (400mg/m<sup>2</sup>), the peak plasma level within 30 min is 8µg/ml [61µM, Kubo, Based on these plasma concentrations in vivo the 1990). following drug concentrations were selected; 0, 1, 5, 10, 20, 50,  $100\mu$ M 5-FU  $\pm$   $100\eta$ M HA. The cell lines MDA-MB-468, MDA-MB-231, and MDA-MB-435 were grown as specified above in examples 4 to 5. When the cultures reached confluence the cells were removed from the flasks in 0.25% trypsin/0.05% The single-cell suspension was counted with a Coulter counter (ZM1 model) and cells were resuspended to 100,000 cells/ml in cell-specific media. Cells were plated into 24-well plates (2cm<sup>2</sup> surface area) by adding 0.5ml of cell suspension per well, resulting in 50,000 cells/well. Cultures were allowed to attach for 24h, before the media was removed, monolayers washed with HBSS and the test media (5-FU+HA) applied. After 4 days of growth in test media the cultures were washed with HBSS, the cells removed from the well by trypsinisation with 0.25% trypsin/0.05% EDTA

15

20

25

and cells were counted with a Coulter Counter.

## Example 8 Evaluation Of HA As A Drug Delivery And Tumour-Targeting Vehicle

Based on the results from the drug sensitivity in vitro experiments as described in examples 5 to 7, and the expression of the HA receptors of CD44 and RHAMM, the human breast carcinoma cell line MDA-MB-468 was selected as the cancer cell inoculant for the generation of any nude mouse human tumour xenografts. Cells were routinely grown and subcultured as a previously described in Example 5. For injection into mice, cells were grown to 100% confluency, trypsinised in 0.025% trypsin/0.01% EDTA solution, washed twice by centrifugation in a Beckman TJ-6 bench centrifuge at 400gav for 10min, counted using a Model-ZM Coulter counter and resuspended in serum-free Leibovitz L-15 medium at 1 x 108 cells/ml.

The athymic CBA/WEHI nude female mice, 6 to 8 weeks old, were maintained under specific pathogen-free conditions, with sterilised food and water available ad libitum. Each mouse received one injection containing 5 x  $10^6$  cells in  $50\mu$ l. The cells were injected with a 26 gauge needle into the mammary fat pad directly under the first nipple (Lamszus et al, 1997). Tumour measurements were made weekly by measuring three perpendicular diameters  $(d_1d_2d_3)$ . Tumour volume was estimated using the formula:

#### $(1/6)\pi$ $(d_1d_2d_3)$

30 Treatment with 5-FU <u>+</u> HA was commenced approximately 4-8 weeks after the cancer cell inoculation. The mean tumour size for mice used in each study is summarised in Table 5.

Table 5:

5

### Summary of Human Breast Cancer Tumours at

Commencement of Each Study

a	•		•	
				• •

Study	Tumour volume	Tumour as % of net body
	(mean + SEM)	mass (mean + SEM)
5-FU targeting	0.41±0.01mm <sup>3</sup>	0.22±0.10mm <sup>3</sup>
Efficacy: 6-	0.37±0.20mm <sup>3</sup>	0.19±0.10mm <sup>3</sup>
week		
Efficacy: 6-	0.61±0.36mm <sup>3</sup>	0.28±0.17mm³
month		

35

To establish the tumorigenicity of breast cancer cell line MDA-MB-468 and its ability to generate tumours upon injection into an appropriate animal host, it was necessary to perform pathological testing. For a tumour to be physiologically viable neovascularisation is essential where the capillary network supplies nutrients to the tumour. The presence of vascularisation, ductal invasion, necrosis, apoptosis, a high mitotic index and nuclear abnormalities are all characteristic of breast carcinoma. Examination of the haematoxylin and eosin stained breast tumour sections demonstrated all of these features, so confirming that the animal host successfully maintained a grade II human breast carcinoma.

Approximately 8 weeks after tumour induction two tumour-bearing mice were given a lethal dose of Nembutal. 15 Within 3min of killing the mice, tumours were surgically removed and immediately fixed in 10% buffered formalin for The fixed tumour was dehydrated overnight in a series of 70-100% ethanol, followed by paraffin embedding from which 2-4  $\mu m$  sections were cut. The sections were placed 20 on slides, de-waxed, and brought to water. Slides were washed 3x5min in PBS. Heterophile proteins were blocked by incubation with 10% foetal calf serum for 10min, followed The detection antibodies were applied for by a PBS rinse. 60min at RT. The detection antisera or antibodies were 25 against RHAMM, CD44H and CAE. The slides were washed 3x5min in PBS and endogenous peroxidase activity blocked by immersion in 0.3% $H_2O_2$  in methanol for 20min. Following a further PBS wash, the peroxidase-conjugated pig anti-rabbit 30 secondary antiserum was applied for 60min at RT, followed by 3x5min washes in PBS. Sigma Fast 3,3'-Diaminobenzidine tablets (DAB) were prepared according to the manufacturer's instructions and the DAB solution was applied for 5-10min The slides were washed in tap water for 10min,

counterstained with haematoxylin, dehydrated and mounted.

The human origin of the tumour was confirmed by staining the tumour and surrounding tissue with a human-

specific cancer marker. The presence of CEA clearly demonstrated that the tumour was human, while being maintained by the cardiovascular system of the murine host. Since it was hypothesised that tumour targeting could occur via receptor-mediated internalisation or binding it was necessary to establish the expression of HA receptors, CD44 and RHAMM. Table 6 lists the degree of receptor expression on the human breast cancer xenografts.

Table 6: Distribution of HA receptors on human breast cancer tumours grown in nude mice

HA receptor	Function	Distribution on	· % epitope
•		tumour	expression or
	Isoforms which bind		tumour
CD44H		Expressed on all	++++
00 1111	and internalise HA	cells except for a	
	(Culty et al, 1992)	few stromal cells	_
CD44 v 6	Functional role in	Some infiltrating	+ .
CD44 Y 0	cancer unknown	tumour cells	
÷.	however the higher		
	the expression		
	results in a		
	diminished survival		
	probability		
•	(Friedrichs et al.	1	
	1995)		
CD // a	Over-expression		
CD44 v 3	often found in breast	. ]	_
•	carcinoma		
	(Friedrichs et al.		
	1995)	1	
<b>50.55.</b> 4. 6. 6. 6.	Necessary for	Groups of	+++
RHAMM	transformation and	infiltrating tumour	• • •
	turnour cell invasion	cells, with high	
	(Hall et al, 1995)	expression on cells	
		surrounding necrotic	
		areas.	
on.	A foctal antigen	Expressed on all	++++
CEA	expressed on	tumour cells	
	malignant cells		
	(Haskell, 1990)	1	

Rating index for percentage of epitope expression on tumour: 0 %:

1-25%: + 26-50%: ++ 51-75%: +++ 76-100%: ++++

15

20

25

#### Example 9 Use Of 5-FU And HA In Nude Mouse Model

Mice were randomly divided into 2 groups of 25 animals. Group 1 received [3H]5-FU only, and Group 2 received the [3H]5-FU/HA combination. The treatments were quantitatively administered via the tail vein with weighing of the injection syringe before and after injection. Tritiated 5-FU (mean injected dpm ± SEM: 31,313,002 ± 131,348) contained within 30mg/kg 5-FU ± 12.5mg/kg HA was delivered in each injection.

To ensure an accurate quantitation of the amount of [3H]5-FU delivered to the blood stream, the injection site on the tail vein was dissected and its [3H]5-FU content measured. The amount of 5-FU delivered to the bloodstream (5-FU available for distribution to the tissues and tumour) was calculated as:

Amount of Dpm/mg of Dpm remaining at Difference in 5-FU mass of x injection injection site delivered injection material to bloodstrea syringe (mg) m (dpm)

The amount of 5-FU delivered to the bloodstream was referred to as the "injected dose".

In order to make accurate comparisons between the sample population and normalise slight variations in organ and tumour masses, the concentration of 5-FU in the body organs and tumour and body fluid was expressed as % of injected dose/gram of tissue.

Mice were individually housed in soft, non-wettable plastic enclosures so urine could be collected. At 10min, 20min, 30min, 1h or 2h after injection mice were anaesthetised by 0.1ml intra-peritoneal injection of Nembutal.

30 Upon anaesthetising the animals, blood was collected from the heart or great vessels using a needle and syringe. Blood was collected into EDTA glass tubes and plasma was prepared by centrifugation at 14,000gav for

35

10min. Radioactivity was counted in 50µl after decolourisation with 100µl of hydrogen peroxide, 30%v/v and the addition of 3ml HiSafeII scintillant. To overcome chemi- and photoluminescence, samples were counted for 2min in a Wallac 1410 ß-counter over a 3, 7 or 20 d period depending on the sample source. During the periods between counting, samples were stored in the dark at ambient temperature. All calculations were performed on stabilised samples where all chemi- and photoluminescence had disappeared. To determine the percentage of injected 5-FU in the plasma, it was necessary to calculate the total plasma volume of each mouse (ml). The standard formula was:

Mouse X mouse blood X plasma proportion Mass (g) volume (0.07) of blood (0.59)<sup>1</sup>

The percentage of injected 5-FU in the plasma was calculated by:

## Plasma volume (ml) X dpm/ml plasma X 100 total dpm injected

When possible urine was collected from the nonwettable plastic enclosures with a syringe and needle. The
urine was cleared by centrifugation at 14,000gav for 10min.

Its radioactive content was measured after the addition of
3ml HiSafeII scintillant to samples ranging from 8-30ul.

Through the technical difficulties in accurately
quantitating the volume of urine produced by each mouse the
% of the injected 5-FU dose in the urine was calculated by
the following formula:

# time of collection (h) x 42µ1¹ x dpm/ul urine x 100 total dpm injected

Once blood was taken, the mice were killed by

10

15

20

25

cervical dislocation. Immediately after killing the mouse the tumour, liver, heart, spleen, bladder, left and right kidneys, uterus, lungs, stomach, intestines, brain and lymph nodes were excised and analysed for total radioactivity. The total radioactivity per tissue was determined by solubilising 100-400mg of tissue in 3-6ml of for 36 h, 22°C. On completion of solubilisation the tissue was counted after adding 10ml of HiSafeIII scintillant. The samples were counted as previously described to avoid chemiluminescence.

As shown in Figure 12, there was a significant targeting effect when combining HA with 5-FU. The greatest relative increase in tumour retention of drug was observed at 10min where the HA enhanced drug uptake by a factor of 2.42 (p=0.001, Students t-test). At 20min and 30min after administration of the HA/5-FU statistically significant increases in the tumour uptake of 5-FU was also noted, with increased drug uptake of 1.5 and 2-fold respectively (p<0.001, Students t-test). The other time points did not demonstrate a statistically significant difference between 5-FU administered as a sole agent versus co-injection with HA.

It was important to establish that metabolic organs such as the liver, spleen and kidneys did not experience a high level of drug targeting which could counter-act any positive aspects of increased tumour targeting. Table 7 lists the [3H]5-FU uptake of each tissue at the various time points tested.

Table 7: Effect of hyaluronan on the biodistribution of [3H15-Fluorouracil in nude mice bearing human breast carcinoma xenografts

-27.

			1111							-
			o-ro	( (				HA/5-FU		-
		mean %	in % dose/g + 1 SE, n=5	1 SE, n=5)			(mean %	$(\text{mean }\% \text{ dose}/9 \pm 1 \text{ SE} \text{ n=5})$	SE n=5)	٠
	10 min	20 min	30 min	1 h	2 h	10 min	20 min	30 min	11	2 h
Tumour	1.49±0.25	2.13±0.28	1.20±0.17	1.34±0.1	1.35±0.24	3.60±0.35	3.20±0.22	2.45±0.14	1.85±0.23	1.03±0.12
Liver	19.64±3.75	23.27±1.6	15.86±3.12	9.20±1.83	3.64±1.09	21.2±1.81	21.37±1.71	21.37±1.71 15.98+1.68	8.73+1.92	3.99+1.24
Spleen	1.45±0.28	1.71±0.18	1.02±0.13	1.02±0.07	0.99+0.09	1.94+0.17	1.39+0.12	1 17+0 20		10.10
Lymph Nodes	2.04±0.31	2.98±0.78	1.49±0.27	1.72±0.46	0.88±0.17	3.47+0.61	2.99+0.47	1 97±0 22	1 85+0 20	01.0±12.10
Kidneys	5,15±1,42	12.53±2.37	10.12±2.01	7.39±1.12	3.97±0.71	9,24+0,9,1	14.56+0.94	14.56+0.94 14.57+1 56 10.72+1 07	10 7241 07	21.0 <del>1</del> 0.12
Bladder	18.30±3.98	18.30±3.98 40.34±26.39 19.11±10.76 33.69±18.72	19.11±10.76	33.69±18.72	61.88±39.1	1	39.17+20.74 37.95+25 1	37.95+25.1	10.72±1.77	5.51±0.98
Intestines	1.33±0.24	1.73±0.42	2.39±0.76	1.57±0.23	2.44±1.42		2.06+0.25	1.90+0.08	1 30± 23	0.010.00.00.00.00.00.00.00.00.00.00.00.0
Stomach	1.59±0.35	1.25±0.40	$1.11\pm0.26$	1.58+0.33	0.76+0.18	2 44±0 52	2.02.0.28	1 62.0 10	C3.TOC.	20.0±7.1.
Brain	0.34±0.02	0.50+0.07	0137+0.06	0.48+0.04	0 55+0 04	O KNED OK	200.330	71.0±0.1	1.30±0.11	1.48±0.02
Heart	1.26±0.21	1.51+0.19	1.01+0.11	0 87.0 05	0000000	1 67 . 0 30	0.00+00.0	00.0+4c.0	0.58+0.04	0.58+0.03
Imac	161+035	2 48±0.45	1.46.0.00	CONTRO	- 1	1.0/±0.20	11.0±00.1	1.03±0.19	1.03±0.19   0.48±0.10   0.36±0.05	0.36+0.05
Dungo	CC.O.Tro.r	C+:OTOT:7	13+0±0±0	Or Otto	0.84±0.01	2.21±0.27	2.23±0.21	2.13±0.19	1.45±0.06	0.92+0.07
Bone	1.37±0.30	1.36±0.13	0.86±0.14	0.89±0.06	$0.86\pm0.18$	2.01±0.07	1.78±0.13	1.18±0.09	1.08+0.19	0.6640.05
Uterus	1.88±0.42	2.52±0.22	$1.63\pm0.24$	1.51±0.24	1.57±0.60	3.38±0.35	3,41±0,47	2.17+0.21	1.78+0.28	1 36±0.45
Plasma	6.26±0.57 5.32±0.	5.32±0.80	2.59±0.20	1.88±0.13	1.36±0.3	2.76±0.18	2.76±0.18 2.76±0.36 2.50±0.28 1.01±0.05	2.50±0.28	1.01+0.05	0.85+0.09
									ı	

12 point bold represents measurements where the co-administration of HA significantly reduced the 5-FU concentration (Students t-test)

represents measurements where the co-administration of HA significantly increased the 5-FU concentration (Students t-test)

20

25

30

35

Figure 13 shows that the primary metabolic organs of HA are the liver, lymph nodes and spleen, while 5-FU is extensively metabolised in the liver.

These organs did not exhibit a significant

increase in 5-FU uptake when it was co-injected with HA.

However, the kidneys did demonstrate a significant increase in 5-FU targeting at 10 min after administration (1.8-fold increase, p=0.004) with HA. After this point, even though, not statistically significant, this trend of enhanced drug uptake continued until the end of the sampling period.

The bladder, intestines and bone marrow did not demonstrate an increased uptake of 5-FU. In tissues such as the uterus there was a short-term increase in drug uptake at 10 min (1.8-fold increase, p=0.032), but no differences were demonstrated at other time points, so the significance of this observation must remain uncertain.

The stomach, brain and lungs did demonstrate increased 5-FU uptake at one or two sampling points. However, due to the small number of animals at each time point (n=5) it was not possible to substantiate statistical significance, even though a definite trend could be observed as shown in Figure 14A-C.

At the later sampling points of 1h and 2h a significant decrease in cardiac 5-FU was noted, where coadministration with HA resulted in a decrease of 59% (p=0.003) and 53% (p=0.021) respectively.

It was not possible to collect urine from each mouse, through variations in the micturition rate; therefore insufficient urine was collected to enable statistical analysis.

When 5-FU was co-injected with HA there was an early decrease in the circulatory levels of 5-FU (Table 7). Hyaluronan reduced plasma 5-FU by 55% (p=0.001). The pharmacokinetic plasma half-life was altered from 28min to 56min in mice receiving 5-FU/HA as shown in Figure 15.

One of the most commonly used treatment regimens for human breast cancer is cyclophosphamide, methotrexate and 5-fluorouacil which is administered on day 1 and 8 of a 28 day cycle. In human breast cancer the initial treatment regimen is for 6 cycles at which time the patient condition is re-assessed, therefore we tried to simulate the human treatment regimen as closely as possible by exposing the mice to 6 cycles (6 months) of treatment in a long term efficacy study and a 6 cycles (6 week) short term efficacy study. Considering the life cycle of a mouse is approximately 2 years we commenced both short-term and long-term treatment protocols as shown in Table 8.

Table 8: Treatment Administration Protocols.

		6-Week Study:	6-Month Study:
Treatment	Dosage	Treatment Regimen	Treatment Regimen
Group		Bolus injection	
Group		on Days	
1. Saline	0.1ml of	1 & 2 of 7 day	1 & 8 of 28 day
	0.9% saline	cycle	cycle
	(injection		_
	grade)		
2. 5-FU/HA	0.1ml	1 & 2 of 7 day	1 & 8 of 28 day
	containing:	cycle	cycle
	30mg/kg		
	5-FU + 12.5		
	mg/kg HA		
3. HA	0.1ml	1 & 2 of 7 day	1 & 8 of 28 day
	containing:	cycle	cycle
	12.5mg/kg		
	НА		
4. 5-FU	0.1ml	1 & 2 of 7 day	1 & 8 of 28 day
	containing:	cycle	cycle
	30mg/kg		
	5-FU		<u>,</u>
5. HA	0.1ml	1: HA	1: HA
followed by	containing:	2: 5-FU	2: 5-FU
5-FU	12.5mg/kg	3: HA	8: HA
	HA or	4: 5-FU	9: 5-FU
	30mg/kg	of 7 day cycle	of 28 day cycle
	5-FU		
6. HA	0.1ml	1: HA	
	containing:	3: HA	
	12.5mg/kg	of 7 day cycle	
	НА		
7.	0.1ml	2: HA	:
5-FU	containing:	4: HA	
	30mg/kg 5-	of 7 day cycle	)
	FU	<u>l</u>	

Mice were randomly divided into 7 groups of 8 animals per group for the short term study and 5 groups of 8 animals for the long term study (refer to Table 8 for dosage and treatment administration schedule).

The treatment was not extended over the 6 month regimen since it has been demonstrated that chemotherapy lasting more than six months has not generally been associated with greater benefit (Harris et al, 1992).

on the day of treatment application for long term study as described in Example 8. In the 6-week study animals were weighed and tumour volumes measured on a daily basis.

Animals were individually placed in an injection box, and the injections were administered via the tail vein. It has been experimentally proven that stress can be a major factor in a patients response to chemotherapy (Shackney et al, 1978), therefore we ensured that equal numbers of mice were allocated to each cage, the animal number per cage varied from 5-8 depending on the stage of experimentation.

The experimental end-point occurred when the animal had to be euthanised due to degree of disease progression or when the 6 month (long term) or 6 week (short term) treatment regimen was completed. Due to the animal ethics guidelines the animals were monitored fortnightly by an independent animal ethics officer who assessed the degree of disease progression. As shown in Figure 16, the following criteria were used to determine if an animal had reached the stage of experimental end-point of necessary death:

- animal was not eating or drinking and had experienced dramatic weight loss;
  - 2). tumour size was greater than 10% of body
    mass (Panel A);
- 3). tumour mass was so large the animal was 35 immobilised (Panel B).

At the experimental end-point the animals were anaesthetised by a 0.1ml intra-peritoneal injection of

10

15

20

25

30

35

Nembutal (60mg/ml), blood was collected followed by killing of the animals using cervical dislocation.

At the end of the 6 week study tumour mass was determined and both the 5-FU and 5-FU/HA therapies had significantly smaller tumours than the saline group (p=0.005) as seen in Figure 17. There was not a significant difference in tumour volume between the 5-FU and HA/5-FU treatment groups, indicating that both therapies displayed equal efficacy against the primary tumour. No statistical difference was noted between the primary tumour volume of saline and HA.

Immediately after killing the mouse the tumour, liver, heart, spleen, bladder, left and right kidneys, uterus, lungs, stomach, intestines, brain and lymph nodes were excised and placed in 4% formalin buffered with 0.06M phosphate pH 7.5, and cetylpyridinium chloride, 1.0% w/v. The tissue was fixed for 16-24h before histological processing. Fixed tissue was dehydrated stepwise to 100% ethanol and embedded in paraffin blocks from which 2-4µm sections were placed on glass microscope slides. Staining the tissue sections with a haematoxylin nuclear stain and eosin cytoplasmic stain highlighted any pathological features that could indicate treatment toxicity.

Nine to 11 lymph nodes were collected per animal, ensuring that all nodes which drained the tumour area were collected. There are currently two methods used for the detection of lymph node metastasis:

- i) routine haematoxylin and eosin staining of gross organ structure
- ii) immunohistochemistry using a cancer marker such as carcinoembryonic antigen

Both methods of metastasis detection were employed in this study. Not all commercially available CEA antibodies react with human breast cancer cells, so we tested the reactivity of 5 different antibodies (DAKO, Amersham and KPL).

The haematoxylin and eosin stained lymph nodes

were examined by Dr P. Allen (certified pathologist) where each node was microscopically examined for the presence of tumour cells. The CEA immunostained lymph nodes were microscopically examined, where any positively stained nodes were counted and considered positive for lymph node metastasis.

Tumour volume was monitored on a daily or weekly basis by calliper measurements and tumour volume calculated as previously described in example 8.

One of the most common toxic effects of 5-FU is on the gastro-intestinal tract where haemorrhagic enteritis and intestinal perforation can occur (Martindale, 1993). Animals were monitored daily for GI tract upset such as diarrhoea and weekly for more severe toxicity

15 manifestations such as weight loss. Weight loss was monitored by calculating net body weight as estimated by subtracting tumour weight, which was calculated as 1g x tumour volume (cm³) as cited in Shibamoto et al, 1996. For demonstration of any weight changes the animal body weight was normalised to the body weight at the time of treatment commencement as:

## Body mass (ex tumour) – body mass at commencement of treatment (ex tumour) Body mass at commencement of treatment (ex tumour) X 100

No daily GI tract upset such as diarrhoea was 25 noted in any of the animals regardless of treatment regimen. Severe gastro-intestinal toxicity for each treatment regimen was estimated using loss of body weight (excluding the tumour weight) as an indicator. At the time of death of each animal the percentage change in body mass was calculated as previously described. There was a 30 statistically significant difference in the normalised body weight between the saline, HA, 5-FU treatment groups as compared to the 5-FU/HA group treatment group (Figure 18). The mice receiving the 5-FU/HA adjuvant therapy demonstrated a 16% increase in body weight (students t-35 test, p=0.025) throughout the treatment in comparison to

10

the untreated group which experienced a net increase of 2% in weight.

The combination of immunohistochemical detection of carcinoembryonic antigen (CEA) with classical diagnostic pathology provided an excellent quantitation of lymph node metastasis. The average mouse contains 15-19 lymph nodes (Lamszus et al, 1997), therefore this study examined approximately 60-70% of the animals lymph nodes. Careful procedure was followed to ensure that all nodes that drained the mammary fat pad and chest region were removed and examined. As demonstrated in Table 9A, all animals displayed lymph node metastasis.

OOGGORGE, CHITCH

The Effect of 5-FU/HA Adjuvant Therapy on the Growth and Metastasis Table 9A

of Human Breast Cancer Xenografts in Nude Mice: 6-Week Study

Treatment	TOT	% of animals	Number of new	% of lymph node	Number of	% change in Lad
Group	Mean±	with lymph	tumours	involved per	animal	weight
	SEM	metastasis		animal mean ± SEM	completing treatment	mean ± SEM
1. Saline	9.4 ± 1.1	100	3	94.2 ± 2.8	8/8	100.1+0.61
2. 5-FU/HA	20.9 ± 2.7	100	0	12.1 ± 0.9	8/8	116.0±0.56
3. HA D1,2	27.7 ± 5.2	100	0	18+41	8/8	10.0 ± 0.00
4. S-FU D1,2	32.1 ± 3.5	100		142+20	0/0	102.3 ± 0.38
5. HA followed hy 5-FI	148+37	To be occepted		C:7 T C:+1	0/0	97.5 ± 0.73
	7.0.7	TO DC assessed	I o oe assessed	To be assessed	8/8	101.8 ± 0.93
6. HA D1,3	30.7 ± 4.9	To be assessed	To be assessed	To be assessed	8/8	1000+036
7. 5-FU D 2, 4	15.3 ± 2.5	To be assessed	To be assessed	To be assessed	8/8	06.5 ± 0.55
					5	70.5 H U./3

10

15

20

25

30

35

Figure 19A shows that the percentage of lymph node involvement (number of metastatic nodes per animal) was greatly affected by 5-FU, 5-FU/HA and HA treatment, where the saline group demonstrated a 6-fold increase in the amount of lymph node involvement. Once again, HA demonstrated that it could have therapeutic value.

While dissecting the animal at the end of the study every tissue was microscopically and macroscopically examined for tumour nodules. With the exception of the mice receiving the HA/5-FU or HA therapy, new tumours were observed around the neck or underarm region of the area adjacent to the primary tumour. The incorporation of HA into the treatment regimen inhibited new tumour formation, as shown in Figure 19B.

There was not a significant difference in overall patient survival regardless of treatment (Table 9A), where animals from all groups completed the treatment regimens.

As one of the major toxicities associated with 5-FU treatment is depression of the bone marrow and subsequent drop in white blood cells it was necessary to assess any treatment associated blood toxicity. Upon anaesthetising the animals, blood was collected from the heart or great vessels using a needle and syringe. Estimation of white blood cell number by making a 1/10 dilution of blood in mouse tenacity saline (M) and counting it on a haemocytometer. A differential blood count was performed by counting neutrophils, lymphocytes, and erythrocytes. The total estimation of blood cell subpopulations was compared to published data for mouse blood.

To ensure that treatments did not induce organ atrophy or enlargement, the organs were removed and weighed during the post mortem. The mass of each organ was calculated as a % of the overall net body weight, and compared to the organ masses of the saline only group (Group 1).

 $f \in$ 

### Example 11 Long-Term Treatment: 6-Month Regimen

While this study is still on-going there are significant data being generated.

- The TDT is the time taken (days) for a tumour to double in mass or cell number, a parameter of tumour growth which is simple to measure and can be easily related to clinical tumour behaviour in conceptional terms (Shackney et al, 1978). By monitoring the tumour doubling time it is often possible to evaluate tumour chemotherapeutic
- 10 response, as slowly growing tumours tend to respond poorly to chemotherapy (Schabel, 1975).

The tumour doubling time for each treatment is shown in Table 9B.

The Effect of 5-FU/HA Adjuvant Therapy on the Growth and Metastasis Table 9B

6-Month Study
; in Nude Mice:
ដ
Cancer Xenografts
Cancer
Breast
of Human
of

			The state of the s
Treatment	TDT Mean± SEM	Experimental endpoint	I umour pathology: Observations
Saline	13.0± 4.0	87.5% immobilsed	No specific characteristics
		12.5% metabolic stress	
5.FII	22.7 ± 2.9	62.5% immobilsed	No specific characteristics
		37.5% metabolic stress	
S-FII/HA	28 ± 2.6	25% immobilsed	Small areas of necrosis appeared, followed by large areas of scab formation. 2/8 tumours
		75% metabolic stress	fully necrosed and dropped oil
HA	26±1.75	100% immobilsed	Small areas of necrosis and scab formation
HA	13.5 ± 0.63	37.5% immobilsed	No specific characteristics
followed by		62.5% metabolic stress	
5-FU			

10

15

. 20

25

There was not a significant difference in TDT between the 5-FU/HA and 5-FU treatment. As with the 6-week study, the administration of HA also demonstrated a therapeutic effect on the primary tumour, demonstrating a TDT of 26+1.75 versus the saline of 13+4 days. The administration of HA 24h before 5-FU appeared to counteract any therapeutic value of 5-FU in relation to retardation of tumour growth.

Tumour mass and volume are useful parameters in monitoring tumour treatment response and progression, but do not ultimately demonstrate the cytotoxic effects rendered by a therapy. We wanted to establish if the HA/5-FU therapy killed more tumour cells and the location of the cells. Dying cells can be pathologically manifested by:

i). disintegration of the nucleus (apoptosis)

ii). lysis of the cell (necrosis)

Scanning the entire tumour image into an MCID computer that calculated the entire tumour area quantitated the number of dying cells. The cells with fragmented nuclei or lysed cells were outlined and scanned, these areas which are then digitised and the exact area of dying cells calculated. The percentage of the tumour attributed to dead cells was calculated by:

## area of apoptotic and necrotic cells X 100 area of entire breast tumour

A viable cell contains more water than a dying or dead cell, therefore by determining the ratio of dry tumour mass to wet tumour mass it is possible to estimate the overall area of viable versus non-viable cells. The tumours were dissected bilaterally where half was processed for tumour pathology and the remaining half was weighed before and after drying at 50°C for 48h. The dry mass as a percentage of wet tumour mass was calculated by:

Dry tumour mass X 100
Mass of wet breast tumour

35

10

15

20.

25

The overall patient survival time was calculated as the time (days or weeks) that the animal lived after the commencement of treatment.

The tumour doubling time for each treatment is shown in Table 9A. There was not a significant difference in TDT between the 5-FU/HA and 5-FU treatments. However, the administration of HA demonstrated a therapeutic effect on the primary tumour, where the TDT was significantly greater than the saline group (p,0.05, Multiple comparison Tukey test). The administration of HA 24 before 5-FU appeared to counteract any therapeutic value of 5-FU in relation to retardation of tumour growth.

The cited cure rate for 5-FU is 26% (Inaba et al, 1989), but the animals receiving 5-FU did not experience a "cure". Two mice receiving the HA/5-FU adjuvant therapy experienced a "cure" where the tumours fully necrosed and dropped off after approximately 12 weeks of treatment. Figure 20B shows the characteristic appearance of small scab formation on mice receiving treatment with HA and HA/5-FU, while Figure 20C shows the appearance of small areas of necrosis followed by the formation of a large area of scab. One of the mice experienced the re-growth of a small nodule, but the second mouse was still tumour free at 22 weeks. seen in Figure 20A, mice receiving 5-FU or saline had large tumours that ultimately ended with the animal dying due to mass of tumour burden (Table 9B), but mice receiving HA + 5-FUdisplayed a characteristic tumour appearance, where a small area necrosed followed by the formation of a scab.

At week 22, 37.5% of the 5-FU/HA mice were still surviving, and the major cause of death for the 5-FU/HA adjuvant therapy mice was loss of weight and metabolic stress (Table 9B).

There appears to be a significant difference in overall patient survival when HA + 5-FU is administered to mice bearing human breast cancer xenografts. At week 22 of a 24 week study the only surviving groups are the 5-FU/HA

30

35

and HA groups, as shown in Figure 21.

### Conclusions

The data from the 5-FU targeting show that there

5 was a statistically significant increase in 5-FU uptake by
tumours when 5-FU was injection with HA at the time points
10, 20 and 30 minutes with a 2.4, 1.5 and 2 fold increase
respectively in 5-FU uptake (Table 7). This indicated that
5-FU was being targeted to the tumour by the HA. There are
two possible mechanisms of HA targeting of 5-FU to tumour
cells:

HA containing associated 5-FU binds to the receptors (CD44) and is internalised via receptor-mediated endocytosis, so releasing the drug into the tumour cell.

The HA molecular mesh will act as an impedance to outward diffusion, so that after HA binds to receptors (CD 44 and RHAMM), the entrained 5-FU is able to diffuse into the tumour cells. While held at the surface of the cells by the HA matrix the 5-FU has increased availability to the active transport mechanism normally utilised for 5-FU transport into the underlying cell.

The catabolism of HA mainly occurs in the lymph nodes (Fraser et al, 1988) and the liver (Laurent et al, 1986). HA is normally cleared from the blood stream by receptor-mediated cellular uptake and catabolism in the \_\_liver (80-90%), kidneys (10%), spleen (0.1%) and bone marrow (0.1%)." (Fraser et al, 1983). Circulating HA is taken up by the metabolic receptor, also known as the liver endothelial cell (LEC) receptor (Eriksson et al, 1983), whereas the CD44 receptor appears to be involved with HA internalisation associated with cellular processes instead of metabolism, while the RHAMM receptor is only involved in cell motility. Combining HA with 5-FU could result in high levels of 5-FU being targeted to the sites of HA or 5-FU metabolism. The data from the targeting experiments (Table 6) shows that there was no significant increase in 5-FU targeting to the liver when administered with HA.

15

20

25

30

observed increased targeting to the liver was observed it could suggest that the LEC receptor on the liver might have a lower binding affinity for HA in comparison to the CD44 receptor. Another possibility is that the CD44 isoform expressed on liver cells (Stamenkovic et al, 1991) does not bind HA with a high affinity. As with the liver no increased targeting of 5-FU was noted in the other metabolic organs of the spleen, bone marrow and lymph nodes.

There was a significant 1.8 fold increase in 5-FU targeted to the kidneys within a 10 min time frame. Although the other four time points did not show a significant increase in 5-FU uptake by the kidney when HA/5-FU was co-administered, there appeared to be a general trend occurring, where more 5-FU delivered to the kidneys on administration with HA. The main pathway for the final elimination of 5-FU from the body is urinary excretion. Even though there seems to be little increase in renal content of the drug with HA, but we believe from other evidence that HA is taken up and catabolised very quickly by the kidneys so that its residence time would be short and associated drug would be quickly released into the urine.

In tissues such as the stomach, brain, lungs and uterus short-term targeting was noted at one or more time points. No consistent pharmacokinetic patterns were generated, which could indicate that we need to increase the population sample number, which could definitively indicate if these observations are genuine. In the case of the increased targeting to the brain at 10-30min this could be explained by the previous observation that. HA has been associated with enhancing the ability of drugs to cross the blood-brain barrier (Nelson & Falk, 1994).

There was a significant increase levels of 5-FU

in the lungs on administration with HA at the time points

min and 1 h. It has been reported that lung macrophages

contain high levels of the HA-binding, CD44 isoform

15

20

(Underhill et al 1993), which could account for the increased targeting. This could be associated with a therapeutic advantage in the treatment of carcinoma of the lung, where small and large cell lung carcinomas have been reported to contain an over expression of CD44 and RHAMM (Horst et al, 1990).

The was a significant decrease in 5-FU targeted to the heart at the 1 and 2 h time points when HA was coinjected with 5-FU. As 5-FU administration can result in cardiotoxicity (MIMS, 1997) administration of 5-FU with HA may reduce the degree of toxicity to the heart compared to when 5-FU is administered alone.

When evaluating the therapeutic efficacy of the HA/5-FU adjuvant therapy several observations were consistent throughout both the long and short-term treatment protocols.

Mice receiving HA/5-FU or HA alone appeared to have more energy and maintain or increase body mass, observations supported by the increased survival times of HA/5-FU mice in the 6-month study.

Tumours of mice receiving 5-FU/HA or HA developed areas of external necrosis, to the extent where 2 tumours dropped off

The addition of HA to 5-FU did not appear to have a significant effect on the volume of the primary treatment 25 · when the therapy was administered for 6 weeks, but this could be due to the vasculature of the tumour. consist of three areas. When HA was administered with and without 5-FU it would reach the tumour, enter the well vascularised and semi-necrotic areas via the large gap 30 junctions of the damaged blood vessels. Due to the ability of HA to absorb water this could result in an influx in extracellular fluid to the necrotic area of the tumour, subsequently increasing the volume of the tumour and causing further damage to tumour vasculature. 35 hypothesis is consistent with the observation that tumours treated with  $HA\pm5$ -FU did routinely demonstrate necrosis and

10

15

20

25

30

35

leakage of tumour intracellular fluid. When the calculation of the necrotic versus viable cell areas and the dry:wet mass ratio is completed we will be able to verify this hypothesis.

The long-term efficacy study showed an increased survival rate for mice receiving HA/5-FU treatment as shown in Figure 21. The mean tumour volume of these mice also appeared to be reduced compared to the other treatment It was also noted in the long term study that the cause of death for the HA/5-FU group was mostly due to metabolic stress whereas cause of death for the 5-FU group was due more to immobilisation due to tumour size being to All the HA only mice died from immobilisation due to the tumour being too large not due to toxicity. does not appear to have any toxicity effects was administered. From the targeting results it was found that increased targeting of 5-FU was occurring when combining HA with 5-FU to the tumour (Figure 12). The ability of HA to target 5-FU to the tumour via HA binding to the HA specific receptors CD44 and RHAMM, which have been showed to be present in increased amounts at tumours sites (Culty et al, 1994; Wang et al 1996), may reflect that the use of HA with 5-FU and other cytotoxic drugs may help overcome the problem of not enough drug reaching the tumour to have any It was also found that in the short therapeutic impact. term study that the 5-FU/HA mice showed a significantly increase in body mass compared to all other groups (Figure 21). Consequently the targeting ability of HA to tumour sites may decrease the amount of 5-FU going to other organs such as the intestines and in so doing reduce treatment side effects associated with 5-FU therapy in particularly gastrointestinal toxicity.

In comparison to the earlier evaluation of MTX/HA adjuvant therapy disclosed in examples 1 to 3, we noted some distinct common results and differences as summarised Table 10.

TOE GET THE STORY OF THE ENGINEER OF THE STORY OF THE STORY

osassia .czisc

Table 10:

# Common Results And Differences Between Adjuvant Therapy With MTX/HA And 5-FU/HA

5

::.: - ~ · . ·

- <del>1</del>	The state of the s	
Study	Similar Results	Different Results
MTX/HA: 6-month	Mice receiving HA/drug	
vs	experienced	,
5-FU/HA: 6-week	significant weight	
<b>*</b> *.	gain; No marked	
	increase in patient	-
	survival; Inhibited	
	formation of new	
	tumours; Demonstrated	
	a longer TDT; Reduced	
<del></del>	lymph node metastasis	
MTX/HA 6-month	Demonstrated a longer	5-FU/HA mice demonstrate
· Vs	TOT	increased survival
5-FU/HA 6-month		
HA control for		HA mice in the 5-FU/HA
MTX/HA: 6 month		study demonstrated that
vs		HA exerted a therapeutic
HA control for		effect by reducing TDT;
5-FU/HA: 6 week		HA reduced lymph node
& 6 month	,	metastasis and tumour
		formation.

10

15

20

25

30

35

The main difference in the two studies was the starting mass of the tumours, where in the MTX/HA study the mean tumour volume 175.13mm³ compared to 61.63 mm³ in the 5-FU/HA study. Through the dynamics of particle movement in to tumours and the response of a patient to the tumour bulk, this could account for the different results obtained in relation to the TDT estimations.

## Example 12 Therapeutic Efficacy Of Combination Therapy With Hyaluronan

One of the most commonly used treatment regimens for human primary and metastatic breast cancer is combination chemotherapy with cyclophospamide (Cyc), MTX and 55-FU which is administered on day 1 and 8 of a 28 day cycle. The combination therapy, often called CMF, is usually given in 6 cycles at which time the patient condition is re-assessed. The antitumour response rate with CMF therapy has been reported to be approximately 50% (Bonadonna, 1981; Bonadonna, 1988), but the therapy has many associated side-effects such as fatigue, nausea, leukopenia and vomiting (Bonadonna, 1976; Meyerowitz, 1979). Due to the success of utilising HA as a drug delivery vehicle for both MTX and 5-FU we evaluated the therapeutic efficacy and toxicity of the HA/CMF adjuvant therapy over a 6-week and 6-month treatment regimen.

The MTX and 5-FU were prepared as previously described in Examples 2 and 6, respectively. The stock concentration of Cyc was prepared by dissolving 1g of lyophilized drug in 1ml of injection grade pyrogen free distilled water and made up to 50ml with injection grade 0.9% sodium chloride. The stock solution was aliquoted into small volumes and frozen at-20°C until used.

A CMF injection was prepared by taking the appropriate volume of the drug stock solution to achieve the final drug concentrations of:

30mg/kg 5-FU (Stock solution: 20mg/ml) 15mg/kg MTX (Stock solution: 24.5mg/ml) 26mg/kg Cyc 12.5mg/kg HA

(Stock solution: 20mg/ml)
(Stock solution: 10mg/ml)

To establish the therapeutic efficacy and any possible toxicities of the CMF/HA adjuvant therapy, human breast tumour xenografts in nude mice were utilized. To simulate the human treatment regimen as closely as possible, mice were treated in 6 cycles (6 months) of treatment in a long term efficacy study and a 6 cycles (6 week) short term efficacy study. Mice were randomly divided into 7 groups of 8 animals per group for the short term study and 5 groups of 8 animals for the long term study.

Mice were treated with 30mg/kg 5-FU; 15mg/kg MTX; 26mg/kg Cyc ±12.5mg/kg on either days 1 and 2 of a 7 day regimen for 6 weeks, or on days 1 and 8 of a 28 day regimen for 6 months. Control groups consisted of the administration of saline, 12.5mg/kg HA or mice who had 12.5mg/kg HA day 1 followed by CMF on day 2. Mice were monitored daily for any treatment toxicity and tumour mass was measured on a daily or weekly basis (see Table 11).

Table 11: Treatment Administration Protocols

:		6-Week Study:	6-Month Study:
Treatment	Dosage	Treatment Regimen	Treatment
Group		Bolus injection	Regimen
·		on Days	
1. Saline	0.1ml of 0.9%	1 & 2 of 7 day	1 & 8 of 28 day
	saline	cycle	cycle
	(injection		
	grade)		
2. CMF/HA	0.1ml	1 & 2 of 7 day	1 & 8 of 28 day
	containing:	cycle .	cycle
	30mg/kg 5-FU		
	15mg/kg MTX		
	26mg/kg Cyc +		
	12.5mg/kg HA		
3. HA	0.1ml	1 & 2 of 7 day	1 & 8 of 28 day
	containing:	cycle	cycle
•	12.5mg/kg HA	·	•
4. CMF	0.1ml	1 & 2 of 7 day	1 & 8 of 28 day
	containing:	cycle	cycle
	30mg/kg 5-FU		
	15mg/kg MTX		
·	26mg/kg Cyc		
5. HA	0.1ml	1: HA	1: HA
followed	containing:	2: CMF	2: CMF
by CMF	12.5mg/kg HA	3: HA	8: HA
	or	4: CMF	9: CMF
	.30mg/kg 5-FU	of 7 day cycle	of 28 day cycle
	15mg/kg MTX		
	26mg/kg Cyc		
6. HA	0.1ml	1: HA	
,	containing:	3: HA	
	12.5mg/kg HA	of 7 day cycle	

As shown in Tables 12a and 12b, in the 6-week study the following was observed:

- 1). Mice receiving a treatment regimen containing HA (CMF/HA, HA followed by CMF or HA only) displayed an
- increased survival of 50% over the CMF only group. The mean survival time for the CMF treatment group was 40.4 days versus 42 for all of the other groups.
  - 2). Animals treated with a combination of HA and CMF all demonstrated a significant weight gain (t-test,
- 10 p<0.001) over animals treated with CMF only or HA only and demonstrated an enhanced well being. (see Figure 22).
  - 3). Tumour doubling time of the saline treated mice (no treatment control group) was significantly less than the other treatment groups (t-test, p<0.001), but there was
- no statistically significant difference between the other treatment groups (see Figure 23).
  - 4). There was a significant difference (t-test, p=<0.001) between CMF and CMF/HA treatment groups with regard to the end-point volumes of the primary tumours,
- where CMF resulted in a reduction in tumour mass in 7/8 animals, while CMF/HA reduced primary tumour bulk in only 3/8 animals.
  - 5). No treatment toxicities were noted when mice were treated with HA  $\pm$  CMF, while mice treated with CMF only
- 25 demonstrated signs of fatigue, conjunctivitis, general poor health.

When the CMF/HA or HA therapy was administered on day 1 and 8 of a 28 day cycle, the following was observed; There was not a significant difference in survival times

- 30 between treatment groups
  - 1). There was not a significant difference in weight gain between treatment groups.
  - 2). The primary tumour of mice receiving HA+CMF exhibited small areas of necrosis and scab formation
- 35 3). In the treatment of the primary tumour, CMF as a sole agent did not demonstrate therapeutic efficacy over the saline and HA treatments. The addition of HA to CMF

OGESTEL CELECE

The Effect Of CMF/HA Adjuvant Therapy On The Growth And Metastasis Of Human Breast Table 12A:

Cancer Xenografts In Nude Mice: 6-Week Study

Treatment	TDT Mean +	\$ of	Number	% of lymph	Change in	Survival	Number of	& change in
Group	SEM	animals	of new	node	primary	time (Days)	animals	body weight
		with lymph	tumours	involved	tumour	mean # SEM	completing	mean ± SEM
		node		per animal	volume (% of		treatment	
		metastasis		mean 1 SEM	original			
					tumour			
					volume)			
					mean ± SEM			
1. Saline	9.4 ± 1.1	100	3	94.2 ± 2.8	494.7+101.6	42+0	8/8	100.1 ± 0.61
2. CMF/HA	29.3 ± 6.2 N/A	N/A	N/A	N/A	30.2+26.5	42+0	8/8	108.7 ± 0.62
3. HA	27.7 ±	100	0	18 ± 4.1	238.0+77.6	42+0	8/8	102.5 ± 0.38
01,2	5.2							
4. CMF	37.6 ± 4.4	N/A	N/A	N/A	-46.2+12.0	40.4+0.68	4/8	84.5 ± 1.37
01,2		•						-
5. HA	21.8 ± 5.8 N/A	N/A	N/A	N/A	55.6+26.6	42+0	8/8	106 ± 0.51
followed								
by CMF								
6. HA	30.7 ±	N/A	N/A	N/A	66.1+30.0	42+0	8/8	100.9 ±
01,3	4.9							0.56

ogogenos.cutsor

Table 12B:

The Effect Of CMF/HA Adjuvant Thorapy On The Growth And Metastasis Of Human Breast

Cancer Xenografts In Nude Mice: 6-Month Study

Tumour pathology: Observations	No specific	No specific	characteristics Small areas of	necrosis by week 11 on 2/8 mice; then large areas	of scab formation. Small areas of necrosis & scab	ion	
Tumor	No Sp	No sp	Chara Small	necro 11 on then	of sc. Small necros	formation	
Experimental endpoint	87.5% immobilised	stress 100% metabolic	stress 100% metabolic	stress	100% immobilised		
Primary tumour volume change (% of original tumour volume)	mean # SEM 494.7±101.6	392.8+129.6	2100.5±564.6		1929.1±661.0	55.6±26.6	66.1+30.0
% of original body mass at experimental end-point Mean	+ SEM 98.569 ± 3.31	90.9 ± 5.44	93.6 ± 4.92		104.6 ± 4.45		
SEM	18.1± 0.39	10.5 ± 0.33	12.6 ± 0.21		18.1 ± 0.45		
TDT Mean ±	14.8± 1.1	40.1 ± 4.0	23.5 ± 1.4		24.7 ± 0.7		
Treatment	Saline	CMF	CMF/HA		на		

**25**.

30

35



resulted in significantly larger (t-test, p=0.001) primary tumours.

The following conclusions can be drawn from this study:

- 5 1). The long-term administration (6-month) of HA/CMF adjuvant therapy does not demonstrate an increase in therapeutic efficacy or a reduction in treatment side-effects.
- A short-term administration (6-week)
   administration of HA/CMF adjuvant therapy demonstrates numerous advantages over the administration of CMF as a sole treatment.
  - 3). Significant weight gain.
  - 4). 50% increase in number of animals completing
- 15 treatment
  - 5). Abolition of side-effects such as fatigue, conjunctivitis, loss of appetite
  - 6). Mice receiving HA did not exhibit any signs of toxicity.

# Example 13 NMR Investigations Of The Nature Of The Interaction Of Chemotherapeutic Drugs And HA

To further investigate the nature of the interaction between HA and chemotherapeutic drugs <sup>1</sup>H Nuclear Magnetic Resonance (NMR) spectroscopy was used. Deuterium oxide (<sup>2</sup>H<sub>2</sub>O (99.96%)) was obtained from Cambridge Isotope Laboratories. MTX was obtained from Faulding Pharmaceuticals and 5-FU and HA stock solutions were prepared as described previously.

Spectra were recorded at 298 K on a Brüker DRX spectrometer operating at 600 MHz with a shielded gradient unit. The 2D experiments were recorded in phase-sensitive mode using time-proportional phase incrementation for quadrature detection in the t<sub>1</sub> dimension (Marion & Wüthrich, 1983). The 2D experiments included TOCSY sequence using a MLEV-17 spin lock sequence (Bax & Davis, 1985) with a mixing time of 120 ms; NOESY (Kumar et al.,

10

20

25

1980) with mixing times of 250 and 400 ms and ROESY spectrum with a mixing time of 250 ms. Temperature calibration of the probe was achieved by comparison to ethylene glycol chemical shifts. All chemical shifts (ppm) were referenced to the methyl resonance of 4,4-dimethyl-4-silapentane-1-sulfonate (DSS, 0 ppm).

Solvent suppression of the water signal for NOESY, ROESY and TOCSY experiments was achieved using a modified WATERGATE sequence (Piotto et al., 1992) in which two gradient pulses of 1 ms was applied on either side of a binomial 3-9-19 pulse. Spectra was routinely acquired over 6024 Hz with 4096 complex data points in  $F_2$  and 512 increments in the  $F_1$  dimension, with 32 scans per increment for the TOCSY experiments and 80 scans for the NOESY.

Slowly exchanging NH protons were detected by acquiring a series of one-dimensional (1D) spectra acquired over 16K data points and with 32 scans.

NMR diffusion experiments were acquired on a Brüker AMX spectrometer equipped with a gradient control unit operating at 500 MHz. All experiments were acquired with 16 or 64 scans at 298 K over 16K of data points and 7575 Hz. A gradient strength of 15.44 G/cm was employed for the diffusion experiments. Each diffusion experiment was obtained from a series of 12 PFGLED spectra in which the delays ( $\tau$ =20 ms,  $\Delta$ =50 ms,  $\tau$ =30 ms and  $\tau$ e = 14 ms) and where the magnitude of G was held constant but the length of the field gradient pulse ( $\delta$ ) was incremented in 1 ms steps from 0.2 ms to 12.2 ms in the final spectrum.

All spectra were processed on a Silicon Graphics

Indigo workstation using Xwinnmr (Bruker) software. For
the 2D experiments the t<sub>1</sub> dimension was zero-filled to 2048
real data points, and 90° phase-shifted sine-bell window
functions were applied prior to Fourier transformation.

The NMR experiments were designed to monitor the

35 changes in the <sup>1</sup>H NMR spectrum of MTX on addition of HA.

By monitoring specific changes in the spectrum of the drug

MTX, such as the broadening or movement of peaks it is

possible to see which regions of the drug molecule, if any interact with HA. Figure 24 shows the 1H NMR spectrum of the MTX dissolved in H2O. This spectrum readily identifies each group of hydrogens in the methotrexate.

5

10

15

20

25

30

35

### Methotrexate

Methotrexate has a number of functional groups that could potentially interact with the hyaluronan molecule. The primary amine moieties on the 2,4-aminopteridine aromatic ring of MTX could form an ionic association with the carboxyl groups on the hyaluronan molecule. Hydrogen bonding interactions between amine groups on methotrexate and the hydroxyl group on the carbohydrate rings of hyaluronan are another possibility. Hydrophobic interactions are also possible between the hydrophobic aromatic rings of MTX and hydrophobic patches on the folded hyaluronan polymer. These interactions are illustrated in Figure 25.

To address the question of whether there was a specific interaction between the methotrexate and HA NMR experiments were designed to monitor the changes in the 'H NMR spectrum of MTX on addition of HA. Figure 26 shows the 600 MHz spectrum of hyaluronic acid at 600 MHz and 298 K.

Figure 27 shows the 600 MHz <sup>1</sup>H NMR spectrum of MTX alone and MTX with increasing additions of HA (50 kDa) of 2 nmoles, 10 nmoles, 20 nmoles and 80 nmoles at 298 K. These spectra show that there is no change in the chemical shift position of any of the peaks in methotrexate. Additional peaks appearing the spectrum as successive amounts of HA is added are entirely consistent with resonances due to hyaluronic acid. Since there is no change in the chemical shift position of any of the resonances of MTX in these spectra it appears that there is no specific region of the MTX molecule that is interacting with the HA molecule.

One way of determining if there is a strong interaction between the NH groups on the MTX and the acid

10

15

20

25

30

35



groups on the HA is to measure the exchange rate of the NH These hydrogens are labile and able to exchange rapidly with the bulk solvent. If however, they are involved in a strong interaction with the HA molecule then they would be protected from the bulk solvent and their exchange rate would be decreased. In this experiment the amine hydrogens of MTX exchange with the deuterium from the  $D_2O$  and the rate of exchange should provide an qualitative estimate of the strength of the interaction between the MTX <sup>1</sup>H NMR analysis of a solution prepared by addition and HA. of deuterium oxide to a solution of MTX and HA dissolved in 0.5% w/v  $Na_2CO_3$  (pH 9) showed that within 4 minutes all amine hydrogens of MTX had exchanged with the deuterium in the sample. This result suggests that the amine hydrogens in MTX are not protected from exchange with the bulk solvent.

The reason that the amine hydrogen peaks disappear from the <sup>1</sup>H NMR spectrum is because deuterium has a very different resonance frequency than hydrogen and therefore doesn't appear in <sup>1</sup>H NMR spectra. Analogous experiments are routinely used to test whether the backbone amide hydrogens in polypeptide and proteins are protected from solvent. When amide hydrogens of proteins are involved in the hydrogen bonding arrangements that stabilize  $\alpha$ -helix and  $\beta$ -sheet secondary structure the exchange rate of these hydrogens is often decreased dramatically. In some cases the hydrogen signals involved in these interaction can persist for hours days or even months depending on the strength of the interaction and it's protection from bulk solvent (for instance in a hydrophobic core of a protein).

Diffusion experiments were performed MTX alone and in the presence of the HA. These experiments could indicate whether the diffusion of the entrapped MTX is retarded by the presence of the HA framework. The results of duplicate <sup>1</sup>H NMR diffusion experiments indicated that for the vast majority of MTX molecules there was no

15

20

25

30

35

retardation of the rate of MTX diffusion since there was negligible difference between the diffusion coefficients of MTX and MTX in the presence of HA. This finding could suggest that in the HA framework there are large solvent cavities between the HA molecules that allows the drug to diffuse freely in this medium.

The diffusion experiments suggested that the bulk of the MTX molecules are free diffuse throughout the HA framework. This scenario does not take into consideration if a small proportion (say 5% of MTX molecules) are interacting weakly in a non-specific manner to the HA molecules.

From the previous experiments it is clear that MTX does not interact strongly with HA and the interaction, if any, is not specific. One way to test weakly binding ligands (10<sup>-3</sup>-10<sup>-7</sup> M) for non-specific binding is to run transferred NOESY experiments. In these 2D experiments crosspeaks will appear if the ligand binds weakly to the macromolecule HA. A transferred NOESY spectrum of MTX/HA showed no crosspeaks due to binding of the MTX to HA which suggests negligible interaction between MTX and HA.

As a further check of whether a small proportion (say 5% of MTX molecules) are interacting weakly in a non-specific manner to the HA molecules. The peaks in a ROESY spectrum should show whether there is even a small proportion of MTX molecules in chemical exchange between free and bound states to the HA. A 250 ms ROESY spectrum did not show any chemical exchange peaks which suggests that not even a small percentage of the MTX interacts with the HA.

### 5-FLUOROURACIL

Figure 28 shows the 600 MHz <sup>1</sup>H NMR spectra of 5-FU and 5-FU (1.25 mg/mL, 1.6 mg/mL and 6.4 mg/mL) with HA (750 kDa, 3 mg/mL) between 70.0 and 8.5 ppm, at 298 K. Initial experiments to investigate whether there was an interaction were performed with 50 kDa hyaluronic acid. No



interaction was observed between the 5-FU and HA (data not To investigate whether an interaction was dependent on the molecular weight of HA used further titration experiments were performed with 750 kDa

- The concentrations of 5-FU utilized are hyaluronan. equivalent to the HA/5-FU adjuvant therapy Kings College London formulation studies which were conducted in preparation for the Swedish clinical trials. concentrations were designed to simulate the concentrations
- used in mixing of HA/5-FU, in the infusion bag and also the 10 HA/5-FU concentration estimated in plasma. Unfortunately, the amine resonances of 5-fluorouracil exchange rapidly ... with the bulk solvent water at the pH (8.8 to 9.1) of these formulations and therefore these resonances are not visible
- in the spectrum of the 5-FU. Only one resonance of CH is 15 visible in the spectrum of 5-FU. Lowering of the pH of these solutions is not feasible since the 5-FU will precipitate out of solution at lower pH values. spectra show that there is no change in the chemical shift
- position of the CH peak of 5-FU. These spectra indicate 20 that the 5-FU does not appear to be interacting with the HA molecule.

Diffusion experiments were performed 5-FU alone and in the presence of the HA. The results of duplicate <sup>1</sup>H NMR diffusion experiments shown in Table 13 indicate that 5-FU diffusion is not retarded by the presence of hyaluronan because there is negligible difference between the diffusion coefficients of 5-FU alone and 5-FU in the presence of HA.

## Table 4: NMR Diffusion Coefficients

sample	HA stock (750 kDa, 10mg/mL)	5-FU (20 mg/mL	Diffusion coefficient m <sup>2</sup> /s
4		62.5 µL	$9.245 \times 10^{-10}/8.900 \times 10^{-10}$
1	300 μL	62.5 µL	$8.701 \times 10^{-10}/9.030 \times 10^{-10}$
5		80 hT	$9.141 \times 10^{-10}/9.204 \times 10^{-10}$
2	300 µL	80 hr	$8.948 \times 10^{-10}/9.021 \times 10^{-10}$
6	-	320 µL	$9.004 \times 10^{-10}/8.997 \times 10^{-10}$
3	300 µL	320 µL	$8.851 \times 10^{-10}/8.833 \times 10^{-10}$

5

2D experiments, NOESY and ROESY: 2D experiments on 5-FU are not possible since only one resonance is visible in its  $^1\text{H}$  NMR spectrum.

NMR analysis of MTX and 5-FU in the presence of
hyaluronan has using titration experiments, deuterium
exchange experiments, diffusion experiments and transferred
NOESY experiments for MTX, and titration experiments and
diffusion experiments for 5-FU have shown that no
interaction could be detected between the chemotherapeutic
drugs and hyaluronan. These recults contract the

drugs and hyaluronan. These results suggest that entrapment of the chemotherapeutic drugs by the hyaluronan network is sufficient to increase the amount of drug delivered to the pathological site. These results are in total agreement with previous studies using gel filtration

chromatography, equilibrium dialysis and CD spectroscopy of the molecular interaction between hyaluronan and MTX and 5-FU which also did not detect an interaction.

osasomo . Osaso

25

### References

Adams JD, Flora KP, Goldspiel BR, Wilson JW, Finley R, Arbuck SG and Finley R, 1993. J. Natl. Cancer.

5 Inst. Monographs 15:23-27.

Akima, K., Ho, H., Iwata, Y., Matsuo, K., Watari, N., Yanagi, M., Hagi, H., Oshima, K., Yagita, A., Atomi, Y & Tatekawa, I. (1996) Evaluation of antitumour activities of hyaluronate binding antitumour drugs: Synthesis,

10 characterization and anti-tumour activity. Jap. J. Drug Targeting 4, 1-8.

Arch R, Wirth K, Hofmann M, Ponta H, Matzku S, Herrlich P and Zoller M, 1992. Science 257(5070):682-685.

Bartolazzi A, Peach R, Aruffo A and Stamenkovic

15 I, 1994. J Exp Med 180:53-66.

Bax, A. & Davis, D.G. (1985) MLEV-17 based two-dimensional homo-nuclear magnetization transfer spectroscopy. J. Magn. Reson. 65, 355-360.

Bissery M, Guenard D and Lavelle F, 1991. Cancer Res 51:4845-4852.

Bisset D, Setanioans A, Cassidy J, Graham MA and Kerr DJ, 1993. Cancer Res 53:523-527.

Bonadonna G (1976) N Engl J Med Med 294: p. 405. Bonadonna G (1981) N Engl J Med Med 304: p. 10.

Bonadonna G (1988) Handbook of Medical Oncology, 3<sup>rd</sup> edition. Chicago, Year Book Med Publ, p. 1075.

Cailleau, R. (1974) Breast cancer cell lines J
Natl Cancer Inst. 55: pp 661-674

Carter D, 1990. Interpretation of Breast

30 Biopsies, Second Edition Raven Press, New York.

Coradini, D., Pellizzaro, C., Miglierini, G., Daidone, M.G. and Perbellini, A. (1999) Hyaluronic Acid As Drug Delivery For Sodium Butyrate: Improvement Of The Anti-Proliferative Activity On A Breast-Cancer Cell Line. Int.

35 J. Cancer. 81:pp.411-416

Culty M, Nguyen HA and Underhill CB, 1992. J Cell Biol 116(4):1055-1062.



Culty, M., Shizari, M., Erik, W., Thompson. and Underhill, C.B. (1994) Binding and degradation of hyaluronan by human breast cancer cell lines expressing different forms of CD44: Correlation with invasive

5 potential. Journal of Cellular Physiology 160: pp 275-286

Dye D and Watkins J, 1980. Br. Med. J 280:1353.

Endicott JA et al, 1989. Annual Reviews in Biochemistry 58: 127-171.

Eriksson, S., Fraser, JRE., Laurent, TC.,

10 Perioft, H. and Smedsrod, B. (1983) Endothelia cells are a site of uptake and degradation of hyaluronic acid in the liver. Exp Cell Res. 144: pp. 223-228

Fraser, JRE., Appelgren, LE. and Laurent, TC. (1983) Tissue uptake of circulating hyaluronic acid. A

whole body autoradiographic study. Cell Tissue Res 233(2): pp285-293

Fraser, JRE., Kimpton, WG., Laurent, TC., Cahill, RNP. and Vakais, N. (1988) Uptake and degradation of hyaluronan in lymphatic tissue. *Biochem. J.* 256: pp. 153-

20 158

Friedrichs G, Folker HJ, Arlt PA and Gunthert U, 1995. The Lancet 345:1237-1238.

Günthert U, 1993. Curr Topics Microbiol Immunol 184:47-63.

Gustafson S, Björkman T, Forsberg N, Lind T, Wikström T and Lidholt K, (1995a). Accessible hyaluronan receptors identical to ICAM-1 in mouse mast tumour cells. Glycoconjugate J. 12, 350-355.

Gustafon, S., Björkman, T., Forsberg, N., McCourt, P., Wikström, T., Lilja, K., Tinner, B., Fuxe, K., Westlin, J.-E., Lidholt, K. Lind, T., Westerberg, G., Bergstrom, M, Langstrom, B., de la Torre, M., Bergh, J., Hagberg, H., Glimelius, B., Lindahl, U., & Laurent, T.C. (1995b) studies on receptors for hyaluronan and the turnover of

35 radioactively-labelled hyaluronan in mice and rats. Royal Soc. Med. Round Table Series n°36, 5-7.

Hall, CL., Yang, B., Yang, X., Zhang, S., Turley,

10

15

20

25

6.00



M., Samuel, S., Lange, LA., Wang, C., Curpen, GD., Savani. RC., Greenberg, AH., Turley, EA. (1995). Overexpression of the hyaluronan receptor RHAMM is transforming and is also required for H-ras transformation. Cell 82: pp

Hardwick C, Hoare K, Owens R, Hohn HP, Hook M, Moore D, Cripps V, Austen L, Nance DM, Turley EA, 1992. J Cell Biol 117(6):pp1343-1350.

Harris, JR., Lippman, ME., Veronesi, U. and Willett, W. (1992) Medical Progress in Breast cancer . The New England Journal of Medicine. 327: pp. 473-480

Hudecz, F., Clegg, JA., Kajtar, J., Embleton, MJ., Pimm, MV., Szekerke, M. and Baldwin, RW. (1993) Influence of carrier on biodistribution and in vitro cytotoxicity of methotrexate-branched polypeptide conjugates. Bioconjugate Chem 4: pp 25-33

Inaba, M., Kobayashi, T., Tashiro, T. and Sakurai, Y. (1988). Pharmacokinetic approach to rational therapeutic doses for human tumour-bearing nude mice. Jpn J Cancer Res 79(4): pp509-516

Klein E.S., He, W., Shmizu, S., Ascula, S., & Falk, R.E. (1994). Hyaluronic acid enhances tritiated fluorouracil uptake in experimental cancer. Royal Soc Med Round Table series no33: 11-15.

Kumar, A., Ernst, R.R. & Wuthrich, K. (1980) Studies of J-Connectivities and selective 1H-1H Overhauser effect in H2O solutions of macromolecules by twodimensional NMR experiments. Biochem. Biophys. Res. Commun. 96 (3), 1156-1163.

Lamszus, K., Jin, L., Fuchs, A., Shi, E., Chowdhury, S., Yao, Y., Polverni, PJ., Laterra, J., 30 Goldberg, ID. and Rosen, EM. (1997) Scatter factor stimulates tumour growth and tumour angiogenesis in human breast cancers in the mammary fat pads of nude mice. Lab Inv 76(3): pp 339-353

Laurent, T.C, 1970. In: Chemistry and Molecular 35 Biology of the Intercellular Matrix. (Editor: Balazs, E.A.) Academic Press, New York. 2: pp. 703-732.

Laurent, TC., Fraser, J.R.E., Pertoft, H. and Smedsrod, B. (1986) Binding of hyaluronate and chondroitin sulphate to liver endothelial cells. *Biochem J.* 234: pp.653-658

5 Lorenz W, Riemann HJ, Schmal A, Schult H, Lang S, Ohman C, Weber D, Kapp B, Luben L and Doenicke A, 1977.

Agents Actions, 7:63-67.

Marion, D. & Wuthrich, K. (1983). Application of phase sensitive two-dimensional correlated spectroscopy

10 (COSY) for measurements of <sup>1</sup>H-<sup>1</sup>H spin-spin coupling constants in proteins. Biochem. Biophys. Res. Commun. 113, 967-974.

Martindale, W. (1993) The extra pharmacopoeia 30th Ed (editor: Reynolds, JEF and Parfilt, K. )

15 Pharmaceutical Press, London

Mathew AE, Mejillano MR, Nath JP, Himes RH and Stella VJ, 1992. J. Med. Chem 35:145-151.

McCourt, PAG., EK, B., Forsberg, N. and Gustafson, S. (1994) Intercellular adhesion molecule-1 is a cell surface receptor for hyaluronan. *J Biol Chem*. 269:pp.30081-30084

McEvoy, 1988. American Hospital Formulary Service-Drug Information 88. Bethesda, MD, American Society of Hospital Pharmacists, Inc. 2222.

Mikelsaar, RH. and Scott, JE. (1994) Molecular modelling of secondary and tertiary structures of hyaluronan, compared with electron microscopy and NMR data. Possible sheets and tubular structures in aqueous solution. Glycoconjugate J 11: pp 65-71

MIMS Medical Network (1996)

http://www.medical.netau/mims-get5-FU/711 Nelson, JA. and Falk, RE. (1994) Anticancer research . Int J Cancer Res Treat

Nikaido N, 1993. Science 264:382-388.

Ogawa Y, Hirakawa K, Nakata B, Fujihara T, Sawada T, Kato Y, Yoshikawa K and Sowa M, 1998. Clin Cancer Res 4(1):31-36.

20

Piotto, M., Saudek, V. & Sklenar, V. (1992) Gradient-tailored excitation for single-quantum NMR spectroscopy of aqueous solutions. J. Biomol. NMR 2, 661-665.

Piper, AA. and Fox, M. (1982) Biochemical basis for the differential sensitivity of human T- and B-Lymphocyte lines to 5-fluorouracil. Cancer Research 42: pp 3753-3760

Rownisky EK, Cazenave LA and Donehower RC, 1990.

10 J. Natl. Cancer. Inst 82:1247-1259.

Schabel, FM. (1975) Concepts for systemic treatment of micrometastases. Cancer 35: pp. 15-24
Scott, JE., Heatley, F. and Hull, WE. (1989)
Secondary structure of hyaluronate in solution. A H-nmr investigation at 300 and 500 MHz in (2H6)dimethyl sulphoxide solution. Biochem J. 220: pp 197-205

Shackney, SE., McCormack, GW. and Cuchural, GJ. (1978) Growth rate patterns of solid tumours and their relation to responsiveness to therapy: An analytical review. Annals of Internal Medicine. 89: pp 107-121

Shibamoto, Y., Murata, R., Miyauchi, S., Hirohashi, M., Takagi, T., Sasai, K., Shibata, T., Oya, N. and Takahashi M. (1996) Combined effect of clininically relevant doses of emitefur, a new 5-fluorouracil

25 derivative, and radiation in murine tumours. Brit. J. Cancer. 74: pp 1709-1713

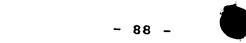
Singh, M., Ghose, T., Kralovec, J., Blair, AH. and Belitsky, P. (1991) Inhibition of human renal cancer by monoclonal-anti-body-linked methotrexate in an ascites

30 tumor model. Cancer Immunol Immunotherapy 32 (50): pp 331-334

Stamenkovic I, Aruffo A, Amiot M and Seed B, 1991. EMBO J 10:343-348.

Underhill, CB., Nguyen, HA., Shizari, M. and
35 Culty, M. (1993) CD44 positive macrophages take up
hyaluronan during lung development. Developmental Biology
155 (2): pp 324-336

اروب د راکشد درسید درسید



Vyas DM, Wong H, Crosswell AR, Casazza AM, Knipe JO and Mamber SW, 1993. *Bioorganic. Med. Chem. Lett.* 3:1357-1360.

Wang C, Thor AD, Moore DH, Zhao Y, Kerschmann R, 5 Stern R, Watson PH and Turley EA, 1998. Clin Cancer Res 4(3):567-76.

Wang, C., Zhang, S. and Turley, EA. (1996) The role of hyaluronan and hyaluronan receptors in breast cancer cell invasion, motility and proliferation. In: Fourth

10 International Workshop on Hyaluronan in Drug Delivery.

(Editor: Willoughby, D.A) Roy.Soc.Med.Press. pp 37-53

Wani MC, taylor HL and Wall ME 1971 7 Am

Wani MC, taylor HL and Wall ME, 1971. J. Am. Chem. Soc 93:2325-2327.

Waugh W, Trissel L and Stella VJ, 1991. Am. J. 15 Hosp. Pharm 48: 1520-1524.

Weiss RB, Donehomer RC, Weirnik PH, Ohnuma T, Gralla RJ, Leyland-Jones B, 1990. Br. J. Clin. Oncol 8:1263-1268.